MATERIAL PROPERTIES OF CHOCOLATE RELEVANT TO TEXTURE PERCEPTION

By

Filippo Bramante

Dissertation submitted to the University of Nottingham
For the degree of Master of Research in Food Science and Engineering

February 2016

Division of Food Sciences
School of Biosciences
The University of Nottingham
Sutton Bonington Campus
Loughborough LE12 5RD, UK

Abstract

The material properties of four texturally different chocolates were investigated with the aim of enabling possible future prediction of texture attributes of chocolate through laboratory protocols rather than human subjects.

The protein profile of the four chocolates was analysed through SDS-PAGE technique. The hardness and the in-water meltdown behaviour of the four chocolates were measured at room temperature and 37°C, respectively, using a Texture Analyser (TA HD Plus, Stable Micro Systems). A stress controlled rotational rheometer (MCR301, Anton Paar) was used to evaluate the apparent viscosity, yield stress and viscoelastic modulus of the chocolates, as well as their friction properties. The chocolates were also emulsified with water to obtain *in-vitro* boluses and their friction properties were evaluated and compared to the respective *in-vivo* boluses.

The chocolates showed different material properties. Two chocolates were harder and more viscous than the other two chocolates which may be due to different amounts of milk fat in the continuous fat phase in the chocolates. The chocolates also showed differences in the meltdown and in the friction behaviour, the latter may be affected by the different particle size of the chocolates. The friction behaviour of the chocolate *in-vitro* boluses was different from that of the respective *in-vivo* boluses, this is supposed to depend on differences in the interface structure between the two types of bolus.

Aknowledgments

I would like to express my gratitude to Dr. Bettina Wolf for her important supervision activity throughout the MRes period. I am also grateful to the project sponsor, Mondelēz, for giving me the opportunity to work on this project. I wish to thank Dr. Qi He for his help with the experimental techniques. Also Dr. Vincenzo di Bari is acknowledged for useful scientific discussions and Dr. Joanne Gould for her suggestions on the writing of this thesis.

Table of Contents

List of abbreviations and symbols

Abbreviations

C-1, C-2, C-3	Commercial chocolate 1, 2, 3
DSC	Differential Scanning Calorimetry
D_{90}	90% particles finer
G'	Storage (elastic) modulus
G''	Loss (viscous) modulus
ICA	International Cocoa Association
IOCCC	International Office of Cocoa, Chocolate and Confectionery
LVR	Linear Viscoelastic Region
MMC	Model Milk Chocolate
PDMS	Polydimethylsiloxane
PGPR	Polyglycerol Polyricinoleate
PSD	Particle Size Distribution
PU	Polyurethane
RPM	Rounds Per Minute
RSD	Relative Standard Deviation
SDS-PAGE	Sodium Dodecyl Sulphate Poly Acrylamide Gel Electrophoresis
w/w	weight/weight

Symbols

α	alpha
β	beta
Δ	delta
η_a	apparent viscosity
μ	friction coefficient

1 Introduction

The sensorial properties of chocolate are related to the chocolate's material properties, which depend on the manufacturing process and recipe. Correlations between instrumental determinations and texture perception have been found and some of the sensory properties of food can be assessed through laboratory methods. Rheological parameters such as apparent viscosity are used during manufacture to predict the final chocolate flow behaviour. Several instrumental measurements on chocolate are performed with the aim of imitating the in mouth behaviour of foods as well as biting and chewing processes, and also to correlate sensory evaluations performed by trained panels with instrumental measurements. The advantages of instrumental measurements include quicker test time than sensory tests and less human resources required and at the same time instrumental measurements exclude any subjective influences on the test. Several sensory properties can be evaluated by instrumental measurements (Winopal *et al.*, 2005).

As defined by the International Standard Organisation (ISO, 1994), texture is "all the mechanical, geometrical and surface attributes of a product perceptible by means of mechanical, tactile, and, where appropriate, visual and auditory receptors". The term mouthfeel is instead normally used in reference to the tactile aspects of texture perception during consumption. Guinard and Mazzucchelli (1999) state that mouthfeel comprises all of the "tactile (feel) properties perceived from the time at which solid, semi-solid or liquid foods or beverages are placed in the mouth until they are swallowed."

The texture properties and the consequent mouthfeel perceptions are related to food mechanical characteristics (hardness, viscosity, brittleness, chewiness, thin, sticky), particles characteristics (gritty, grainy, fibrous) and also moisture and fat content (dry, moist, oily, greasy) (Civille and Szczesniak, 1973; Szczesniak, 1963; Szczesniak, 1979).

A texture analyser is a device used to measure material properties such as hardness, fracturability or adhesiveness, and it can be also used to imitate in

principle the biting or chewing process of a food, providing information about the bite behaviour of different foods. Texture analysers with puncture probes or various penetration dies are also used for hardness and firmness measurements of foods.

A very important texture property of foods is viscosity, which describes the flow behaviour (flow resistance) of fluid products. Rheometers are common devices utilised for viscosity measurements. Correlation between viscosity data and some aspects of perceived texture in the mouth was found by different authors; for example, initial thickness and dynamic viscosity of fluid foods and fluid thickened systems have been correlated by Cutler *et al.* (1983) and Richardson *et al.* (1989).

1.1 Dissertation structure

In the Introduction, the background to material properties and their characterisation applied to chocolate in this research is provided. The physical analysis techniques used to characterize the milk chocolate samples are described (equipment, materials, methods) in the material and methods section followed by the results and discussion of the tests carried out on the chocolates.

1.2 Melting properties

The melting properties of chocolate are related to the crystalline state and proportion of solid fat present in the finished product (Afoakwa *et al.*, 2008a). Differential Scanning Calorimetry (DSC) is used as a tool to characterise the melting properties of chocolate and it measures the relative amounts of each crystalline state (Tabouret, 1987; Walter and Cornillon, 2001; Walter and Cornillon, 2002). It has been observed that the peaks corresponding to latent heat are in the temperature ranges related to melting of specific polymorphic forms (McFarlane, 1999), and it has been seen to affect sensory characteristics and mechanical and rheological properties of chocolate (Hartel, 2001).

1.3 Hardness of chocolate

Hardness is a measure of the physical rigidity (texture) and it is represented by the maximum penetration force measured through the sample. A correlation between the amount of force needed to break the food and the relative perceived hardness was found (Dan *et al.*, 2007; Kim *et al.*, 2012). For chocolate, it has been seen to depend on different factors including recipe, manufacturing technology and cooling temperature. It is a useful indicator of good tempering (Afoakwa *et al.*, 2008b) and it is also related to the sound perceived when the chocolate is snapped and good hardness at its first bite, which are closely linked properties and both important indicators of a high quality chocolate to the consumer.

1.4 Analysis of meltdown

Chocolate melts in the mouth following a complex process. According to Guinard and Mazzucchelli (1999), the melting rate is defined as "the time required to melt half of a - milk - chocolate square when chewed in mouth". The authors described a series of sensory attributes and how variations in sugar and cocoa butter content in chocolate affected those attributes. In particular, they found the samples with high fat content to be faster melting, whilst samples with low sugar and low fat content were more viscous. In sensory studies conducted on chocolates with reduced fat content, a strong negative correlation was found between chocolate melting properties and their perceived thickness, which correlated well with the measured viscosity (Spearing, 2007). A study on consumer liking showed that chocolates with high melting speed in the mouth were preferred to slow melting chocolates (Bolenz *et al.*, 2000). Since sensory perception of melting does not only depend on the chocolate melting speed, but it is also affected by the fluidity of the melted product, chocolate viscosity needs to be maintained as low as possible (Do *et al.*, 2007).

1.5 Rheology

As with most food materials, liquid chocolate is considered a non-Newtonian fluid, which means that its viscosity changes with the shear rate applied. Figure 1 shows the different types of rheological behaviour of fluids. The most common behaviour is called pseudo-plastic or shear thinning behaviour. In this case, the viscosity decreases as the shear rate increases. Pseudo-plastic behaviour is common with fluid materials whose microstructure is a dispersion of micro particles in a continuous fluid. This is the case of chocolate, in which sugar and cocoa solids are dispersed in a continuous fat (cocoa butter) phase. The shear thinning behaviour is due to the orientation of the closely packed particles to the shear field, which cause a reduction of viscosity as the shear rate increases (Wells, 2009). In the case of chocolate, the deagglomeration of the solid particles and the subsequent release of entrapped fat would lower the viscosity.

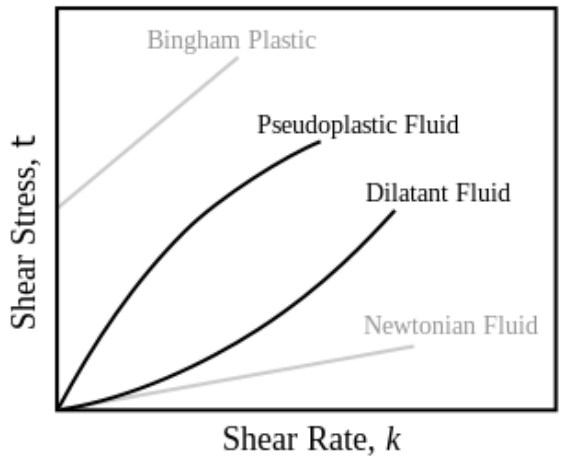

Figure 1: Types of rheological behaviour of fluids. The shear stress is presented as a function of shear rate.

Chocolate rheology is useful to measure as it impacts on the efficiency of process steps in which the chocolate is moved, e.g. mixing and pumping steps (Servais *et al.*, 2004), and also to the final quality and the sensorial characteristics of product (Ahmed and Ramaswamy, 2006; Glicerina *et al.*, 2013). Steady shear and oscillatory rheology are used to characterise food

rheological properties in relation to sensory characteristics like thickness, stickiness and sliminess (Afoakwa *et al.*, 2008b; Malone *et al.*, 2003; Richardson *et al.*, 1989). In chocolate, perceived viscosity has been seen to correlate well with instrumental viscosity and yield stress by Guinard and Mazzucchelli (1999). In particular, the correlation between sensory and instrumental viscosity was highly significant; also the correlation between sensory viscosity and yield stress was significant but to a smaller extent compared to instrumental viscosity. Since instrumental viscosity is measured at higher shear compared to yield value, Guinard and Mazzucchelli (1999) supposed that in the mouth, high-shear rate conditions are produced, due to higher correlation with instrumental viscosity. The perceived viscosity was seen to depend on the fat and sugar contents in the analysed chocolate samples.

In general, studies on the relationship between viscoelastic properties and sensory attributes have been reported. For example, Brighenti *et al.* (2008) found a good correlation between the storage modulus and texture properties such as firmness and stickiness of cheese. Greenaway (2010), in a study on skin cream, reported high correlation between storage modulus and texture properties such as firmness, slipperiness, stickiness and thickness. Although no clear examples of relationship between viscoelastic properties and sensory attributes in chocolate were found so far, oscillatory rheology is a useful technique to provide further information about structural properties in chocolate, like the role of fat content, type and amount of emulsifiers in determining the yield value (De Graef *et al.*, 2011). Taylor *et al.* (2009) used both steady shear and oscillatory rheology to characterize the rheological profile of a milk chocolate. Stress or strain amplitude sweep techniques were used with rheometers fitted with parallel plates or concentric cylinder geometries.

The viscoelastic properties of chocolate, as well as the flow properties, depend on the microstructure of the material. From oscillatory rheology measurements it is possible to get information about the stress at the end of

the linear viscoelastic region (LVR) and the corresponding complex modulus, as well as information on the microstructural arrangement of the sample, showing the existence of a structural network in liquid chocolate that needs to be broken in order to let the chocolate flow (De Graef *et al.*, 2011). The level of interactive forces between particles inside the material influence G'; some authors observed that a high value of G' is related to a high level of interaction between solid particles (Johansson and Bergenstahl, 1992).

1.6 Tribology

The rheological behaviour of food is known to be related to several sensory properties such as creaminess, smoothness, sliminess and thickness. Although food texture in the mouth is seen to be correlated with viscosity, bulk rheology alone cannot provide a clear characterisation of in-mouth sensory properties. At the same time, the microstructure of foods is clearly linked to their physical and rheological properties but the link between microstructure and food organoleptic characteristics is less clear, because the eating process is very complex and it is difficult to replicate that process using objective measurements (Malone *et al.*, 2003).

Tribology (or thin film rheology) is the science which measures the properties of adhesion, friction and lubrication and it has been seen as a useful tool to investigate the characteristics of food materials in thin films that cannot be deduced from bulk properties, and to find correlations between food microstructure and sensory properties (Malone *et al.*, 2003). For tribology measurements, the interfacial properties of materials, thus the interactions between food components and oral surfaces are important.

During chewing, foods undergo grinding and deformation processes and thin food films form between two shearing (teeth) or squeezing surfaces as the tongue and palate (Giasson *et al.*, 1997; Luengo *et al.*, 1997), Several authors used tribological techniques on mayonnaise and chocolate to find correlations between thin film properties and their sensory profile. These materials, during chewing and swallowing, are squeezed between surfaces

(or food substrate and palate) and the surfaces' movement creates a thin film of food whose rheological characteristics are responsible for the oral perception. The authors found that in these foods, thin film tribological measurements gave better correlation with the composition and texture of the samples than the bulk rheological properties (Malone *et al.*, 2003). Correlations between sensory perception and friction instrumental measurements have also been found on different foods or food-like systems. de Wijk and Prinz (2005) measured the friction of vanilla custards and related these measurements to sensations like astringency, roughness and creaminess. Malone *et al.* (2003) related the measured friction of guar gum solutions and sunflower oil with slipperiness and fattiness, whilst Dresselhuis *et al.* (2008) measured the friction of emulsions prepared from whey protein isolate and sunflower oil and related the results to the perception of roughness and fatty mouthfeel. Regarding chocolate, Carvalho-da-Silva *et al.* (2013) related higher instrumental friction to lower sensory mouthcoating.

The tribological behaviour of food samples is normally reported as the Stribeck curve that is a plot of the coefficient of friction μ, which is the ratio of frictional force to load acting perpendicular to two surfaces in contact, on the y axis, against a combined parameter of viscosity, speed and load on the x axis. The Stribeck curve is also more easily expressed as friction coefficient against sliding speed (mm s^{-1}), as shown in Figure 2. A Stribeck curve is normally divided into three regimes: the boundary regime, the mixed regime, and the hydrodynamic regime, representing three very different friction scenarios and, in case of oral processing, the different amount of food sample between the tongue and palate. A further regime, the elasto-hydrodynamic regime, can be observed when the materials undergo elastic deformation during lubrication .

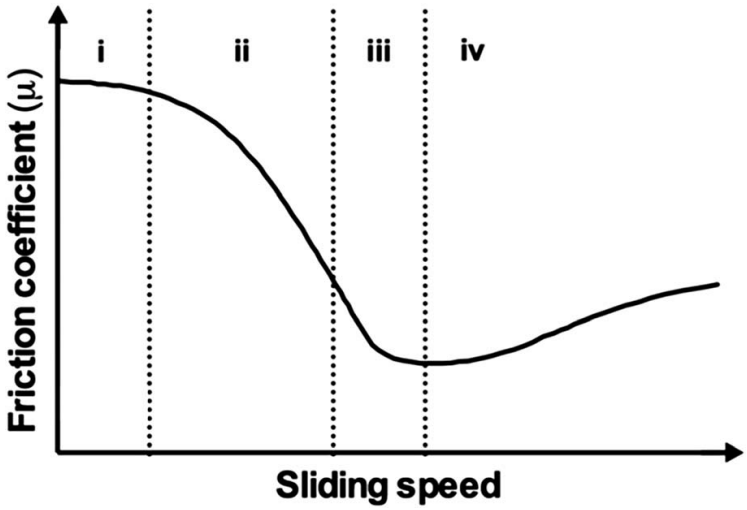

Figure 2: Friction coefficient μ versus sliding speed with four lubrication regimes: (i)boundary regime, (ii) mixed regime, (iii) elasto-hydrodynamic (EHL) regime and (iv) hydrodynamic regime (Carvalho-da-Silva *et al*. 2013).

Food oral perception is known to be linked to the friction between food and oral surfaces especially in the boundary and mixed regimes. In the boundary regime, the sliding speed is not sufficiently high to entrain the lubricant between the two surfaces and the fluid hydrodynamic pressure is insufficient to separate them, so the two sliding surfaces have mechanical contact and this gives high levels of friction. This regime is known as the characteristic of the in mouth situation, because of the low sliding speeds and low contact pressures, and it might be related to the human perception of astringency (Prakash *et al.*, 2013).

With increasing sliding speed there is an increase in the material entrainment in the friction zone and the mixed regime is observed, which is characterised by a progressive reduction in the friction coefficient with increasing sliding speed. In this regime, the food entrainment into the tongue–palate contact zone is able to partly separate the two sliding surfaces, and the surface roughness is roughly equal to the film thickness, so both fluid pressure and asperity contact pressure participate in bearing the contact load (Cassin *et al.*, 2001). This regime is found in mouth during food consumption, when the product is sheared and squeezed to a thinner film.

The characteristics of the oral surfaces (hydrophobic and rough) and the interaction with the lubricant are important in determining the friction behaviour. The creamy-soft sensations, generated by fat, might be related to the mixed regime. The fat covers the oral tissue with a coating thereby reducing the friction between food and oral tissue through lubrication (de Wijk and Prinz, 2005; de Wijk *et al.*, 2003). A significant level of correlation was also found between the sensory perception of slipperiness and the friction in the mixed regime through tribological tests on food hydrocolloids (Malone *et al.*, 2003).

The elasto-hydrodynamic regime is encountered at further increase in the sliding speed, when the contact pressure is sufficiently high to cause elastic deformation of one or both of the surfaces (de Vicente *et al.*, 2005). Here the minimum friction is observed. No examples of correlation between this regime and sensory perception have been discussed in published literature on food tribology.

The hydrodynamic regime is found at even higher sliding speeds. Here, the lubricating film is able to separate the tongue and palate surfaces and it sustains the whole applied load. The friction coefficient increases again, because the food-lubricant viscosity becomes predominant, while the surface characteristics loose importance. In this regime food thickness is sensorial perceived, at the start when food is consumed as the rate of entrainment of the food into the contact zone due to surface motion gives a sufficiently high fluid pressure to completely separate the surfaces (Prakash *et al.*, 2013).

As long as the food layer thickness and fluid pressure is sufficiently high to meet the hydrodynamic regime, rheology would be a relevant approach to understand physical behaviour of food, but this approach becomes less efficient for samples in the mixed and boundary regimes, which would certainly require tribological interpretation (Prakash *et al.*, 2013).

It is very important to consider the impact of the surface on friction data. The friction coefficient measured on soft surfaces was found to depend on

the load applied, this was the case of mucosal surfaces as pig tongue and pig oesophagus; the friction coefficient was instead constant when measured on hard surfaces as glass, metal and rubber (de Hoog *et al.*, 2006).

1.7 Analysis on chocolate bolus

Chocolate is subjected to structural modifications during consumption; it is converted from a dispersion of solids in a continuous fat phase into an oil-in-water emulsion. Food emulsions have been demonstrated to show a certain degree of correlation between viscosity and texture perception. There is often a high degree of correlation between microstructure of emulsions and their physical and rheological properties reported, while the link between food microstructure and its organoleptic attributes is less clear. This is probably due to the difficulties in reproducing the complexity of the eating process with objective measurements (Malone *et al.*, 2003).

Friction properties of chocolate seem to have been linked to texture perception (Carvalho-da-Silva *et al.*, 2013). It is however true that the friction properties of oral processed chocolate could give better correlation with sensory data since the bolus represents the chocolate in the in mouth situation, but friction analysis on the oral processed chocolate may be affected by the subjectivity of the panellists and also the use of biological sample material is involved. These two issues may be overcome by using a chocolate emulsion obtained through a laboratory based protocol (*in-vitro* bolus) instead of the oral processed chocolate (*in-vivo* bolus).

1.8 Aims and objectives

Aims of the study:

- To characterise some of the material properties of four types of chocolate, manufactured by Mondelēz, through the use of laboratory protocols. These characterisations could potentially lead to future prediction of sensory attributes of chocolate through laboratory protocols.

Objectives of the study:

- To determine the hardness of the chocolates samples, which is correlated to first bite force, through the use of a texture analyser;
- To observe the meltdown profile of the chocolate through the use of a texture analyser;
- To evaluate the chocolate rheological properties as well as their friction properties through the use of a rheometer.

2 Materials **and methods**

2.1 Chocolates

The sample set for this research comprised of three commercial milk chocolates and one specifically manufactured milk chocolate labelled C-1, C-2, C-3 and MMC, respectively. The primary ingredients as shown on the packaging for the three commercial chocolates are listed in Table 1 while Table 2 shows the recipe of MMC.

Table 1: Ingredient composition as shown on the packaging of the commercial milk chocolates used in this research

sample →	**C-1**	**C-2**	**C-3**
Ingredient ↓		**%w/w**	
Fat	30.5	30	29.5
Carbohydrates	56.5	56.5	58.5
Protein	7.5	8.4	6.4

Table 2: Recipe* of MMC

ingredient	**%w/w**
Sugar	56.83
Fat	29.48
Non Fat Cocoa Solid	5.12
Protein	6.59
Lecithin	0.55

* values kindly provided by Mondelēz

2.2 Protein analysis

The protein profile of C-1, C-2, C-3 and MMC was determined by SDS-PAGE (Sodium Dodecyl Sulphate – Poly Acrylamide Gel Electrophoresis) analysis.

For protein extraction, first the samples were melted. A 2 g sample of chocolate was placed in a centrifuge tube (Sarstedt) and left to melt in a convection oven (Sanyo, MOV-112F) at 45°C for 40 min. Then, 10 g of a 2% SDS solution, prepared by mixing 2 g of SDS powder (Fisher Scientific) in 98 g of RO water, was added to the melted chocolate.

After dissolution into the SDS solution, the chocolate samples were shaken for 20 minutes in a vortex mixer and then centrifuged (Rotina 380, Hettich Zentrifugen) at 3000 g for 30 min at 4°C to prevent sample overheating during the centrifugation. Three phases were obtained after centrifugation: cocoa solids at the bottom, a liquid phase containing proteins in the middle and a fat phase as upper layer. Afterwards, 100 µL of the liquid phase were mixed with 100 µL of sample buffer, prepared by mixing 95% Laemmli Buffer (Biorad) and 5% β-mercaptoethanol (Biorad) in a 2 mL microtube. This solution was then heated (Stuart Scientific heater) at 95°C for 10 min to denature the proteins, then centrifuged (Heraecus Fresco 21 Centrifuge, Thermo Electron Corporation) for 1 min at 13 g at 4°C and eventually stored on ice.

For the electrophoretic analysis, a prepared gel cassette 4-20% gel percentage Mini-Protean TGX Stain Free Gel, (Bio Radgel; 15 well comb, 15 µL) was used as electrophoresis gel and inserted into a Minitrans Blot Cell (Biorad) linked to a power source (Biorad, model 1000/500). The running buffer was prepared by mixing 10% of 10X Tris/Tricine/SDS Buffer (Biorad) with 90% of RO water. A Precision Plus Protein™ Dual Color Standards (Biorad) protein marker was used as standard to identify the molecular size of the extracted proteins. 10 µL of protein marker and 15 µL of each sample were loaded with a pipettor into the gel spots. For the protein migration, an electric field was applied with the power source at 120 V and 50 mA for 35 min. At the end of the run, the gel was washed with cold water, then

"Imperial Protein Stain" dye (Thermo Scientific) was added onto the gel, previously placed in a 150x20 mm plastic Petri dish (Sarstedt), and left to stain for 2 hours under shaking in a shaking incubator (NB-205, N-Biotec INC) (55 rpm, 20°C). After the staining phase, the dye was removed and the gel was repetitively rinsed with running cold water for 2 hours.

2.3 Melting properties

The melting temperature of the four chocolates was measured using a Pyris Diamond DSC (Perkin Elmer, UK), calibrated for temperature and heat flow using indium at a scan rate of 5°C min^{-1} using an empty aluminum pan as a reference. Following a similar method to (Afoakwa *et al.*, 2008a), samples (~5 mg) were loaded into pans, which were then sealed with lids using a sample press. Pans were heated at 5°C min^{-1} from 5 to 55°C in a N_2 stream. Onset temperature (T_{onset}), peak temperature (T_{peak}), end temperature (T_{end}) and enthalpy of melting (ΔH_{melt}) were calculated using the software provided by Perkin Elmer. Each sample was analysed in duplicate and mean values and standard deviations are reported.

2.4 Hardness measurement

The hardness of the four chocolates was determined using a Texture Analyser (model TA HD Plus, Stable Micro Systems) fitted with a 5 kg load cell. The data were acquired and analysed with the instrument software (Exponent 6,7,1,0). In the following subsections, the different methods used to assess the hardness are reported. A published method (section 2.4.1) and a method provided by the project sponsor (section 2.4.3) were compared. The same method of section 2.4.3 was applied in section 2.4.2 but with opposite orientation of the chocolate piece.

2.4.1 Needle Method

In this method, a similar procedure to Afoakwa *et al.* (2008b) was followed. Here, a penetration needle probe (Stable Micro System, 2mm Cyl/Stainless;

Part Code P/2) attached to an extension bar was utilised; the needle was lowered at pre-test speed of 1.0 mm s^{-1}, test speed of 2.0 mm s^{-1}, post-speed of 10.0 mm s^{-1}, and the maximum penetration distance was 5 mm. Hardness was determined as maximum penetration force (g), of the needle through the chocolate piece from the top of the sample. The analysis was conducted at 20°C; ten replicates per sample were conducted and analysed.

2.4.2 Cone Method – penetration on the chocolate piece top

In this method, the penetration needle was replaced with a Perspex cone (height 38.7 mm, base diameter 30 mm); the pre-test, test and post-test speed were respectively 1.0 mm s^{-1}, 0.5 mm s^{-1}, 10.0 mm s^{-1} and penetration distance was 3 mm. The chocolate piece was placed on its back and the cone penetrated on the top of the piece. The number of replicates was between 6 and 10 depending on the chocolate.

2.4.3 Cone Method – penetration on the chocolate piece back

In this method the chocolate piece was placed on its top and the cone penetrated on the back of the piece. The different chocolate piece orientation in sections 2.4.2 and 2.4.3 was considered to see if the orientation affected the hardness. Penetration on the back is used by the industrial sponsor. The number of replicates was between 6 and 10 depending on the chocolate.

Table 3 shows the size of the chocolate pieces utilised in the hardness measurement; chocolate piece shape and dimensions vary according to type of chocolate. The size measurement was made with a calibre, and ten measurements were performed for each sample. Figure 3 shows a schematic representation of the method used to measure chocolate hardness.

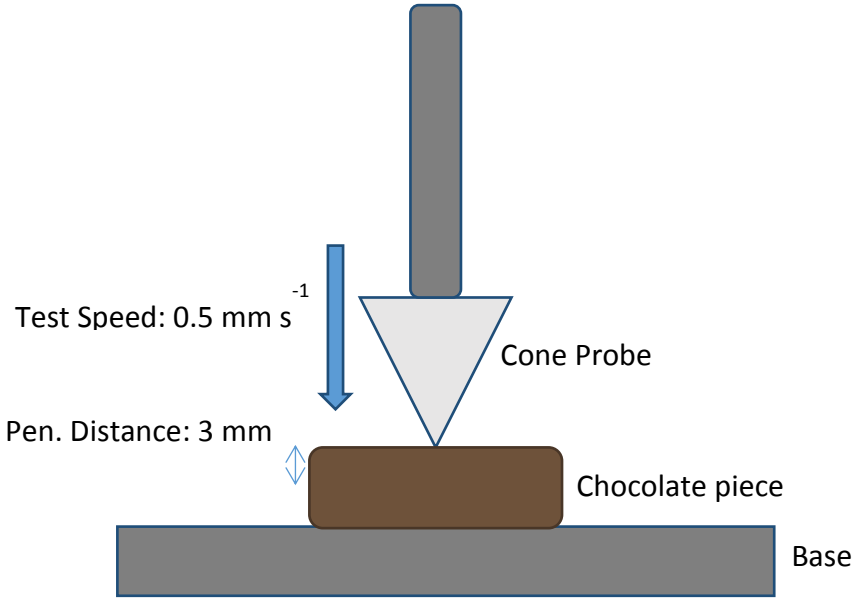

Figure 3: Schematic representation of the cone-probe method used for chocolate hardness measurement, described in sections 2.4.2 and 2.4.3. In the needle method, the cone was replaced with a needle (see section 2.4.1).

Table 3: Dimension of the chocolate piece utilised for hardness analysis

Dimension (mm)	C-1	C-2	C-3	MMC
Width	21	25	18	20
Length	23	27	27	36
Height	11.01±0.24	10.20±0.20	7.66±0.17	9.16±0.54

The parameters for the three types of test are summarised in Table 4.

Table 4: Summary of the parameters of the three types of hardness test

Probe	Pre-test speed	Test speed	Post-test speed	Penetration distance
Needle	1.0 mm s^{-1}	2.0 mm s^{-1}	10.0 mm s^{-1}	5 mm
Cone – Top	1.0 mm s^{-1}	0.5 mm s^{-1}	10.0 mm s^{-1}	3 mm
Cone - Back	1.0 mm s^{-1}	0.5 mm s^{-1}	10.0 mm s^{-1}	3 mm

2.5 Analysis of meltdown

The melting speed of C-1, C-2, C-3 and MMC was determined following the procedure of Spearing (2007). A jacketed stainless steel vessel (120 mm diameter, 155 mm height), with circulating water at 37°C was placed on the measurement platform of a Texture Analyzer (TA HD Plus, Stable Micro System) fitted with a 5 kg load cell (see Figure 4).

Figure 4: Texture analyser equipment setup used for chocolate meltdown measurement (A) fitted with perspex probe, and stainless steel vessel (B) used for the analysis of meltdown.

For the analysis of meltdown, the four chocolate samples were previously cut into a cylindrical shape (12 mm diameter; 8 mm height) with a circle cutter. Small variability in the height of the samples was associated with the

method for sample preparation. The chocolate cylinders were then smeared with grease on the bottom and upper surfaces and placed onto a Perspex platform (65 mm diameter, 6 mm thickness) supported by three cylindrical Perspex legs (20 mm height), as shown in Figure 5.

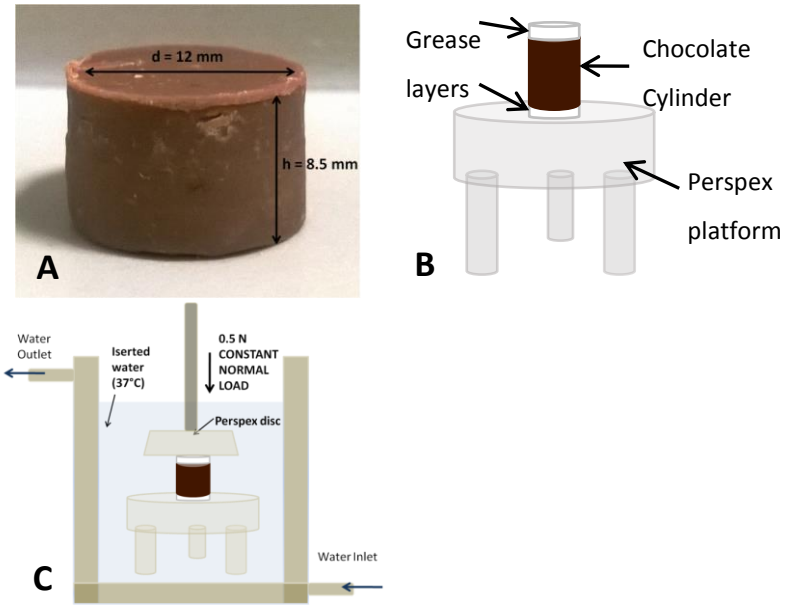

Figure 5: (A) Example of chocolate cylinder prepared for the analysis; (B) Schematic representation of how the chocolate cylinder was placed on the Perspex platform; (C) Schematic representation of the setup used for measuring melting profile, adapted from Spearing (2007).

The Perspex platform with the chocolate cylinder was then inserted into the vessel, and a Perspex compression disc (60 mm diameter, 5-mm thickness) was lowered until reaching the contact with the sample. At that same moment the run was started, the sample was fully covered with 350 mL of water preheated to 37°C, to mimic in mouth temperature. The covering water was kept at constant temperature by the circulating water in the double jacketed vessel; a thermal probe was used to check the temperature of the covering water during the analysis. The force applied on the chocolate cylinder was constant, with a value of 0.5 N, and the trigger force was set at 0.049 N. The test duration was 500 s, after which the probe automatically returned to the start position.

The grease layers smeared on the chocolate cylinder surfaces were used to keep a good contact between sample and Perspex discs and to act as a barrier to water too. The two Perspex discs acted as insulators, so the heat transfer through the sample was considered to be mainly radial.

Spearing (2007) describes the melting conditions as static, in order to emphasize the difference to the dynamic and more complex melting situation that occurs in the mouth during chewing. The shape of the melting curves in this study was characterised by an initial low slope part, followed by a steep steady decrease and reaching a final lower plateau.

In this study, the parameters analysed as relevant to in mouth melting (Do *et al.*, 2007; Spearing, 2007) were:

- *t-start* (s): The time needed for the heat, transferred in radial form, to melt the chocolate cylinder through to the centre, which then starts collapsing. This time is graphically represented by the duration of the initial low slope. It is determined as the abscissa of the intersection between the initial plateau height with the tangent to the slope, as illustrated in

Figure 6.

- *collapse speed*: It is represented by the high slope of the curve and it refers to the speed at which the sample collapses. It is expressed in $mm.s^{-1}$ and calculated as the absolute value of the slope.

- $t_{50\%}$: It is the time (s) at which the chocolate cylinder reaches half of its original height. It is calculated as the abscissa of the intersection between the melting curve and the height line at 4 mm.

All the chocolate samples were analysed in triplicate and the results are expressed as mean and standard deviation.

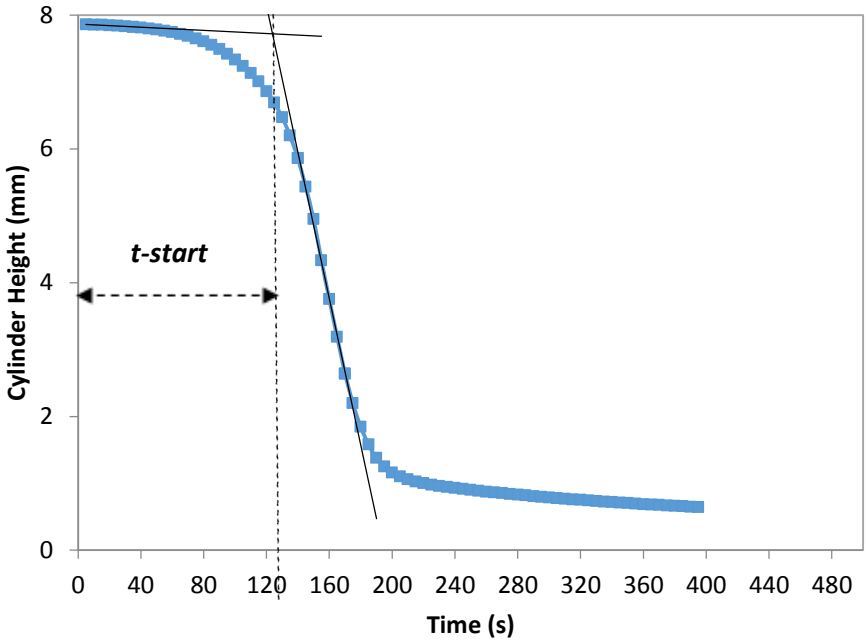

Figure 6: Example of calculation of *t-start* for C-1.

Since the chocolate cylinders were in direct contact with water, possible dissolution of the sugar particles exposed at the surface of the cylinders was considered. In order to test this hypothesis, the volume of a C-1 chocolate cylinder was measured before and after the test and the variation of volume that occurred was considered to depend on the sugar dissolution from the chocolate cylinder. The volume of the melted chocolate was obtained as follows. Since it was reasonable to assume that the melted cylinder at the end of the test had the shape of a disc, the diameter of the disc was measured, while the height of the disc was obtained from the meltdown curve; it was therefore possible to calculate the volume of the melted chocolate at the end of the test. The amount of sugar assumed to be dissolved in water was obtained by multiplying the difference in volume between the chocolate cylinder and the melted cylinder by the sucrose density (1.59 g/cm^3). The amount of sugar in the chocolate cylinder was calculated as the percentage in weight of the sugar over the chocolate cylinder weight. Moreover, with the aim of evaluating how sugar dissolution could affect the meltdown profile of the chocolate cylinders, the meltdown

test was repeated on a chocolate cylinder previously greased on the whole surface in order to avoid direct contact between chocolate and water and consequent sugar dissolution in water. The meltdown test was repeated once for C-1 and once for C-3. Finally, the test was also performed on a solid cocoa butter cylinder obtained through the same procedure used for obtaining the chocolate cylinders, in order to evaluate the meltdown behaviour of the major component of the fatty phase of the chocolate and how the absence of solids could affect the meltdown.

2.6 Rheology

The rheological properties of C-1, C-2, C-3 and MMC were measured using a stress controlled rotational rheometer (MCR301, Anton Paar, Graz, A) fitted with a concentric cylinder geometry (CC27/T200/55/P, diameter 26.66 mm; measuring cup CC27, diameter 28.92 mm, Anton Paar).

2.6.1 Steady shear rheological analysis

Before the analysis, 25 g of each chocolate sample was melted in an oven at 45°C for 45 min and then loaded into the cup, kept at 40°C, before lowering the inner cylinder into the cup. The rheological properties of the melted chocolates were measured according to the International Cocoa Association (ICA) (previously the International Office of Cocoa, Chocolate and Confectionery – IOCCC) guidelines, as follows. The method consists of four steps. In the first step, a preliminary constant shear rate (5 s^{-1} for 500 s) was applied, in order to equilibrate the sample temperature. After that, an increasing shear rate ramp (2-50 s^{-1} in 180 s, 1 measurement each 10 seconds - 18 measurements in total) was applied, then the shear rate was maintained constant (50 s^{-1} for 60 s; 1 measurement each 10 s – 6 measurements in total) before finally decreasing the shear rate (50-2 s^{-1} in 180 s, 1 measurement each 10 seconds - 18 measurements in total) (ICA (former IOCCC (2000)); Wollny, 2005). The temperature of analysis was 40°C.

Each sample was analysed in triplicate and the results are shown as apparent viscosity η_a as a function of shear rate.

Normally, yield stress and apparent viscosity are used to describe the rheological behaviour of liquid chocolate. The yield stress quantifies the energy needed for chocolate to start moving from the rest (Beckett, 2008; Do *et al.*, 2007), and it describes chocolates moulding and enrobing abilities, that happens at low shear rates. The apparent viscosity, instead, describes the chocolate behaviour at high shear rates, typical of pumping and mixing processes.

A standard method recommended by the ICA in the confectionery area consists of reporting the shear stress at 5 s^{-1} as the yield stress (YS5) and the viscosity at 40 s^{-1} as the apparent viscosity (η_{40}) on the ascending shear rate ramp (Do *et al.*, 2007).

2.6.2 Oscillatory rheological analysis (strain sweep)

Before the analysis, the chocolate samples (25 g per replicate) were melted at 40°C for 45 min then gently mixed with a spatula. The CC27 geometry was lowered into the cylinder, after loading it with the melted chocolate.

The strain sweep test consisted in measuring the storage modulus G' and loss modulus G'' as a function of the strain γ (%). Following the method developed by Mondelēz, the strain amplitude in the test was increased from 0.0012 to 10% and a constant oscillatory frequency of 1 Hz was applied.

The impact of pre-shear on the viscoelastic behaviour of the chocolate, as applied for steady shear analysis following recommendations by ICA was evaluated. Pre-shear protocol, if applied, consisted of shearing at 5 s^{-1} for 500 s, followed by starting the strain sweep immediately or after a 60 s period of rest (zero shear). The temperature of analysis was 37°C in order to simulate the in mouth temperature.

2.7 Tribology

The tribological characteristics of the chocolates were evaluated by using a stress controlled rotational shear rheometer (MCR301, Anton Paar, Graz, A), fitted with a commercially available tribology attachment, based on the ball on three plates principle (Anton Paar, Graz, A, BC12-7 tribology cell). Figure 7 shows the tribology equipment used for the tests. A 12.7 mm diameter steel ball (1/2”, 10 PCS. Material 1.4401, Grade 100) and soft plates of 13.5 mm × 6.0 mm × 3.2 mm were used. The chocolates were tested on two different kinds of soft plates, made with two different materials, polyurethane (PU) and polydimethylsiloxane (PDMS). Both materials are hydrophobic, and the role of the surfaces was to mimic (oral) epithelial surfaces. PDMS is often used in food tribological studies because of its high resemblance to the elasticity of human tongue (Johnson *et al.*, 1993). However, since PDMS was thought to swell in contact with a high fat material such as chocolate, the first tests were performed on PU, which is another material used in food tribology (Carvalho-da-Silva *et al.*, 2013). PDMS was tested and the results revealed that it did not swell, instead giving good responses during the test; further tests were then conducted on PDMS rather than on PU, since PDMS is more common in tribology works. A temperature device (H-PTD200, Anton Paar) was used to cover the stage during the measurement to prevent possible temperature variations.

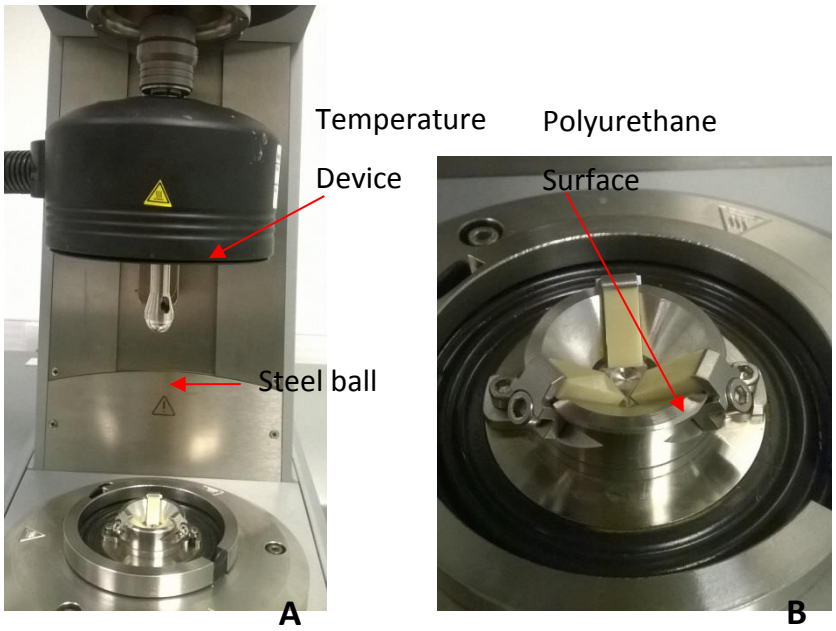

Figure 7: (A) Tribology Equipment with steel ball and temperature device, (B) stage with soft hydrophobic surfaces (in picture the polyurethane surfaces are shown)

PU was obtained from a 3:10 mixture of Isocyanate and Polyol (both Axson Technologies, USA), gently mixed and then poured 3.2 mm high into a plastic Petri dish. The dish was left at room temperature for 1 hour and then placed in the oven for 1 hour at 80°C to cure. Afterwards, the polyurethane was left to cool at room temperature. PDMS surfaces were instead obtained from a two-component elastomer kit (Dow Corming, Michigan, USA), poured 3.2 mm high into a plastic Petri dish then cured in the oven at 65°C for 4 hours and finally left to cool at room temperature. Both the surfaces sets were cut to the desired dimensions using a scalpel.

Before measurement, the chocolate was melted in an oven set at 45°C for 2 hours. After gentle manual mixing, 1.2 g of chocolate was loaded onto the stage before lowering the steel ball into the measuring position. The temperature of analysis was 37°C. Different methods were applied according to the kind of surface used.

2.7.1 Test on PU surfaces

Before starting the tribological measurements on chocolate, the PU surface set was tested with sunflower oil and the test was repeated after each six measurements on chocolate. The surface test with sunflower oil was performed in order to check the consistent performance of the plates during the chocolate analysis.

For the tribological tests performed both with sunflower oil and with chocolate, the friction coefficient μ was measured as a function of sliding speed, which varied from 0.001 to 420 mm s^{-1} in 240 seconds, recording 60 evenly spaced data points (Carvalho-da-Silva *et al.*, 2013). Before that, a preliminary steady shear step (conditioning step) for 10 s at 100 mm s^{-1} sliding speed was applied, followed by a 10 s period of rest (zero shear). The preliminary steady shear step was applied in order to equilibrate the tested material surface film in the friction zone developed through the interaction between the two friction surfaces, so generating a steady state and ensuring some adsorption of the sliding surfaces with lubricant. After the 10 s rest step, two consecutive test runs were applied.

The tests were conducted applying two different constant normal forces, 0.5 N for sunflower oil and 3 N for chocolate (Cassin *et al.*, 2001; Malone *et al.*, 2003) and the results of the 2 consecutive runs are separately reported as friction coefficient versus sliding speed curves, for both tested materials. Each chocolate was analysed in triplicate and the results are shown as means for the three first and three second runs. At the end of each measurement, the surfaces were cleaned with hot water and detergent, then dried and treated with ethanol. The different normal force at which the tests with sunflower oil and chocolate were performed is not relevant because the aim of sunflower oil tests was exclusively that of checking the surface performance over time. However, another series of surface performability tests was carried out at 3 N, in triplicate, after having completed the four chocolates friction tests.

2.7.2 Tests on PDMS surfaces

The friction properties of the four chocolates were also evaluated with PDMS as soft surface. The PDMS surfaces performed consistently when tested with liquid cocoa butter; the measurements were made on the new surface and in between the chocolate tests, using the following parameters: 3 N normal force throughout the test, 10 s conditioning step at 100 mm s^{-1} plus 10 s of rest, test speed from 0.001 to 420 mm s^{-1}, 60 evenly spaced data points in 240 s, 2 consecutive test runs. The chocolates were tested with the same method used for cocoa butter, and 4 replicates per sample were analysed. A further method was also used for testing the chocolate, following a previously published protocol (Carvalho-da-Silva *et al.*, 2013). For this protocol no preconditioning step was applied, and the same type of test run as in the first method was applied 8 times consecutively per sample, 3 replicates per chocolate, and the results are reported as mean of the values of run 8 of the three replicates. The first seven runs of the 8 runs method were used to equilibrate the chocolate surface film in the friction zone developed through the interaction between the two friction surfaces, so generating a steady state (Carvalho-da-Silva *et al.*, 2013).

2.8 Analysis on chocolate bolus

The first step in the in vitro bolus development was determining the amount of water to use for the emulsion. For this, a 2 g piece of chocolate was chewed for 20 s and then expectorated. The expectorated chocolate was weighed, then dried and the dried portion was weighed and assumed to be the quantity of chocolate that is effectively part of the bolus; this quantity was less than the initial 2 g of chocolate, in this way the amount of chocolate lost in the mouth during chewing was taken into account. The difference in weight between the expectorated bolus and the dried chocolate was considered the amount of saliva present in the bolus, thus the water amount that would have been used in the emulsion. As the expectorated chocolate

was then constituted by 44% of chocolate and 56% of saliva, the in vitro bolus was therefore reproduced with this percentage.

The in-vitro bolus was then prepared by melting 18 g of each chocolate in 22.9 g of ultrapure water at 37°C and then emulsified at 6000 RPM for 40 s, by using a disperser (Ultra Turrax, T 18 basic, IKA). Microscope images of C-1, C-2, C-3 and MMC emulsions were taken at 10× of magnitude by using a microscope (AVG-EVOS).

The friction characteristics of the bolus were evaluated following an unpublished *in-house* method for *in-vivo* boluses. A rotational rheometer fitted with a tribological stage and soft plates of PDMS (see section 2.7) was used for the test. 1.5 mL of emulsion were loaded into the tribology stage and previously submitted to a conditioning step at 100 mm s^{-1} for 10 s, followed by a 10 s period of rest. After that, the test run consisted in increasing the sliding speed from 0.1 to 705 mm s^{-1}. The applied normal load throughout the test was 3 N. Three batches for each chocolate were prepared and each batch was used for one replicate, therefore three replicates per chocolate were analysed. The tribological analysis and the microscopy analysis were performed immediately after the emulsions were prepared. Tribological data are expressed as average and standard deviation of three replicates; the friction curves are shown as friction coefficient) as a function of sliding speed.

2.9 Statistical analysis

Average, standard deviation and error bars for the experimental data were determined with Microsoft Excel 2010. Error bars in charts are expressed as ± standard deviation of the experimental data. Relative standard deviation (RSD) is the ratio of the standard deviation to the mean and it is expressed in percentage. The Anova test (Tukey' HSD test) was conducted with IBM SPSS Statistics 22.0.

3 Results and discussion

3.1 Protein analysis

The milk protein profile of the four chocolates obtained with SDS-PAGE analysis is shown in Figure 8.

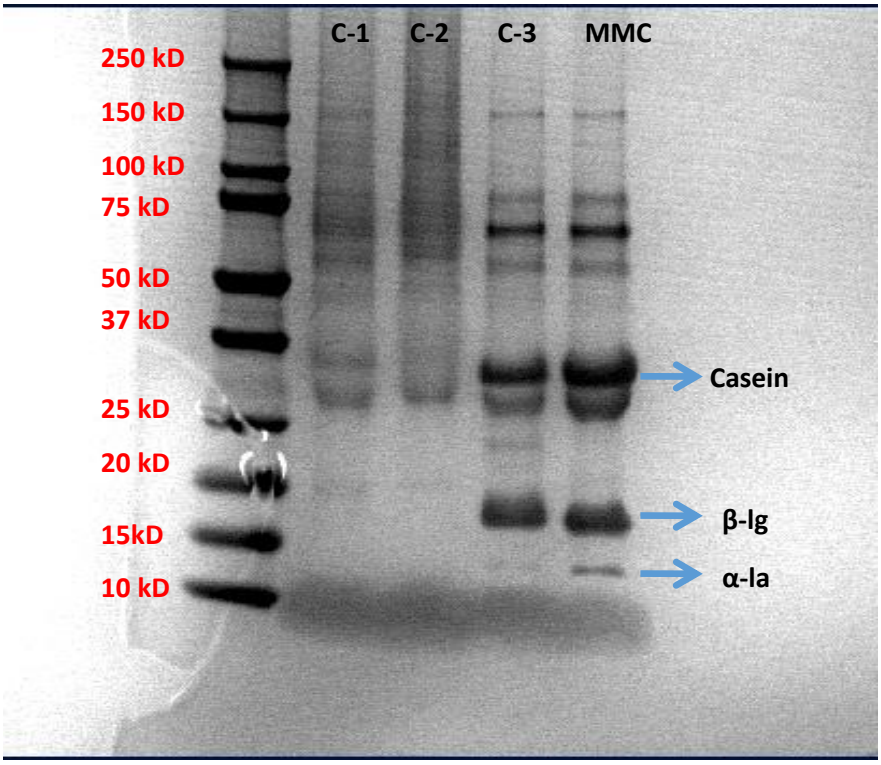

Figure 8: SDS-PAGE profile of C-1, C-2, C-3 and MMC. The protein marker standard is visible in the first spot and the respective band molecular weights are reported.

As depicted in Figure 8, C-1 and C-2 have a different protein profile compared to C-3 and MMC. C-3 and MMC show two bands at around 15 kD, which belong to β-Lg and α-La (Zagorchev *et al.* 2013; Basch *et al.* 1985; Jovanovic *et al.,* 2007) whilst C-1 and C-2 do not show these two bands. The presence of the β-lg and α-la bands for C-3 and MMC indicate a different type of milk ingredient used in the manufacturing process of the four chocolates and can be due to the use of whey powder in the formulation of these two chocolates. All the samples show casein bands, between 25 and 37 kDa (Zagorchev *et al.*, 2013) although they are more visible in C-3 and MMC

than in C-1 and C-2. In bovine milk, four types of caseins are present: α_{s1}-Casein, (molecular weight around 23.5 kDa), α_{s2}-Casein (molecular weight around 25 kDa), β-Casein (molecular weight around 24 kDa) and κ-Casein (molecular weight around 24 kDa) (Farrell *et al.*, 2004). The casein bands of the four chocolates were however observed at higher molecular weight compared to the values provided by Farrell *et al.* (2004). This is probably due to their high hydrophobicity which causes an over-absorption of SDS. As reported by Basch *et al.* (1985) and Green and Pastewka (1976), caseins behave abnormally in SDS-PAGE. From the protein bands shown in the picture it is not possible to clearly distinguish the four types of caseins.

3.2 Chocolate melting properties

In Figure 9, the DSC thermograms are reported for the C-1, C-2, C-3 and MMC chocolates. In Table 5, the values of onset temperature (T_{onset}), peak temperature (T_{peak}), end temperature (T_{end}) and enthalpy of melting (ΔH_{melt}) related to Figure 9 are reported.

The melting temperature of chocolate is related to the melting temperature of the fat, in particular cocoa butter. Cocoa butter is characterized by fat polymorphism, it means that the fat can crystallise in different forms. Taking in consideration the fat crystal forms classification by Wille and Lutton (1966), the most familiar in confectionery industry, six different polymorphic forms are considered, labelled from Form I to Form VI. Forms V and VI are the most stable in cocoa butter, in particular Form V is the most desirable one and the state produced in a well tempered chocolate. The melting temperature of Form V is about 31°C (Le Reverend *et al.*, 2009). As shown in Figure 9, all of the chocolates show a comparable melting profile, which is an indication that the fat in the chocolates is in the same polymorphic form. In particular, the clear melting peak T at around 31°C indicates that the cocoa butter in the chocolates is in Form V. The other two peaks found at lower temperatures are an indication of the melting of milk fat.

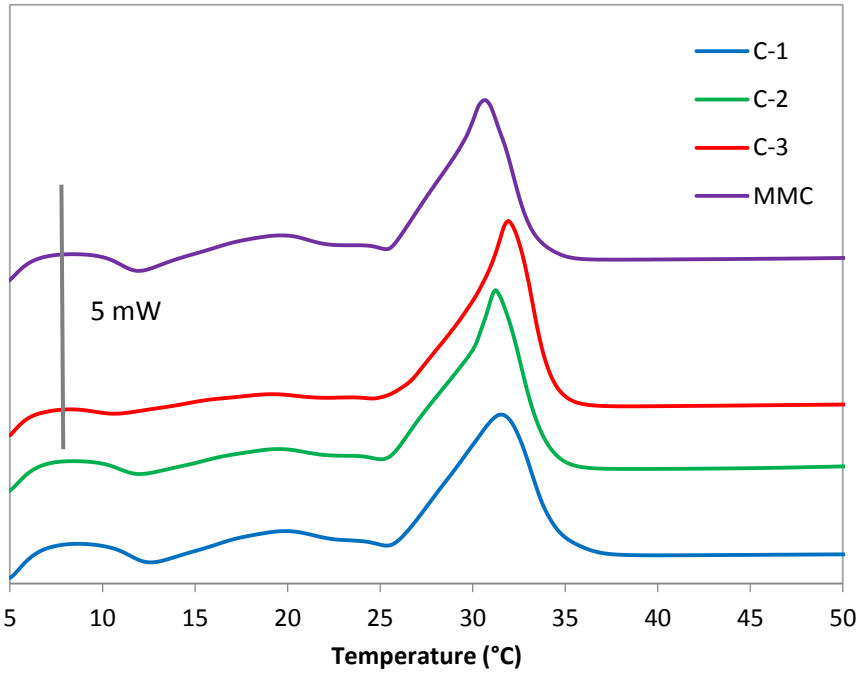

Figure 9: DSC curves of the four chocolates melting

As shown in the table, the melting properties of the four chocolate samples were not significantly different from each other ($p<0.05$), it means that the chocolates tend to melt at the same temperature.

Table 5: Melting properties of C-1, C-2, C-3 and MMC. Samples with same letters indicate no significant difference ($p<0.05$) according to Tukey' HSD test.

Samples	T_{onset} (°C)	T_{peak} (°C)	T_{end} (°C)	ΔH_{melt} (J.g^{-1})
C-1	26.26±0.25^{a}	31.67±0.39^{a}	34.34±0.57^{a}	18.08±1.23^{a}
C-2	28.10±0.11^{a}	31.29±0.03^{a}	33.83±0.16^{a}	21.31±0^{a,b}
C-3	28.62±1.54^{a}	31.74±0.16^{a}	34.26±0.12^{a}	23.64±0.33^{b}
MMC	27.78±0.40^{a}	30.98±0.78^{a}	32.82±0.93^{a}	21.59±2.15^{a,b}

The solid fat content (SFC) is the amount of fat in solid form at a defined temperature. Estimated DSC values of SFC at 20°C of the four chocolates are reported in Table 6. The results are shown as percentage of SFC over the total fat content.

Table 6: SFC at 20°C of the four chocolates, expressed as percentage of solid fat over total fat content. Samples with the same letters indicate no significant difference ($p<0.05$) according to Tukey' HSD test.

Samples	SFC (%)
C-1	$82.48\pm0.04^{a,b}$
C-2	$82.33\pm1.44^{a,b}$
C-3	84.99 ± 0.66^{b}
MMC	81.26 ± 0.44^{a}

3.3 Chocolate hardness

The hardness values measured with the needle method (see section 2.4.1) are shown in Figure 10. The values reported for the four chocolate samples are all statistically different. In particular, C-1 and C-2 show a higher level of hardness compared to C-3 and MMC.

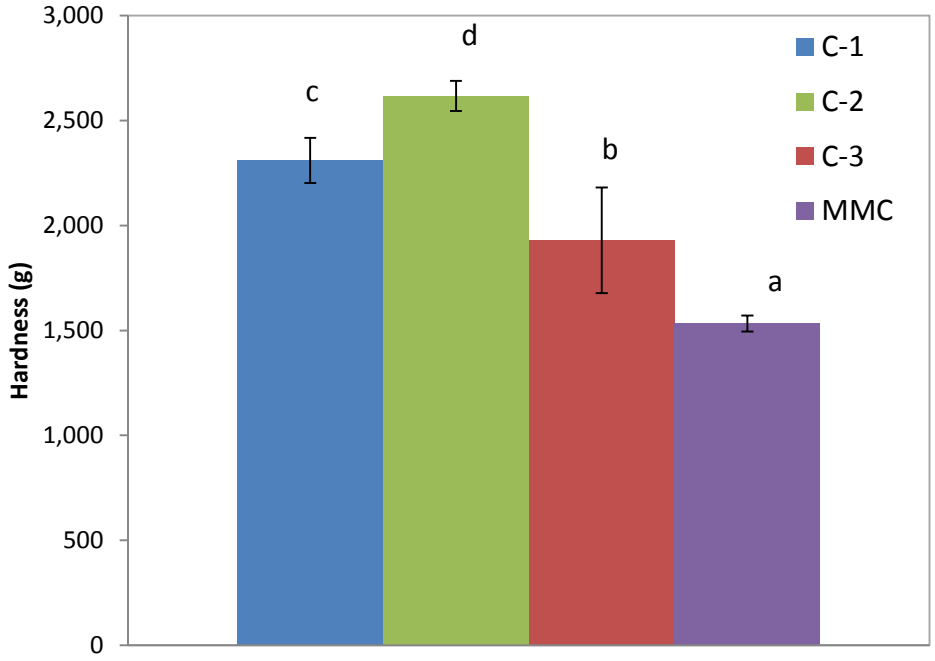

Figure 10: Chocolate hardness measured with the needle probe. 10 replicates per sample for C-1, C-2 and C-3; 9 replicates for MMC. a-d means samples with different letter are significantly different ($p<0.05$) according to Tukey' HSD test.

The higher standard deviation of C-3 compared to the other samples is expected to depend on the micro-fractures that already exist in the product, as C-3 tended to break during the analysis. C-3 broke 4 times over 10 replicates. However, the mean value of hardness is similar between broken and unbroken samples, as illustrated in Figure 11. This figure shows that the sample breakage occurs only after the highest force - hardness - was measured (at about 0.6 s). The chocolate piece breakage is reported as a sudden drop in force before the test ends.

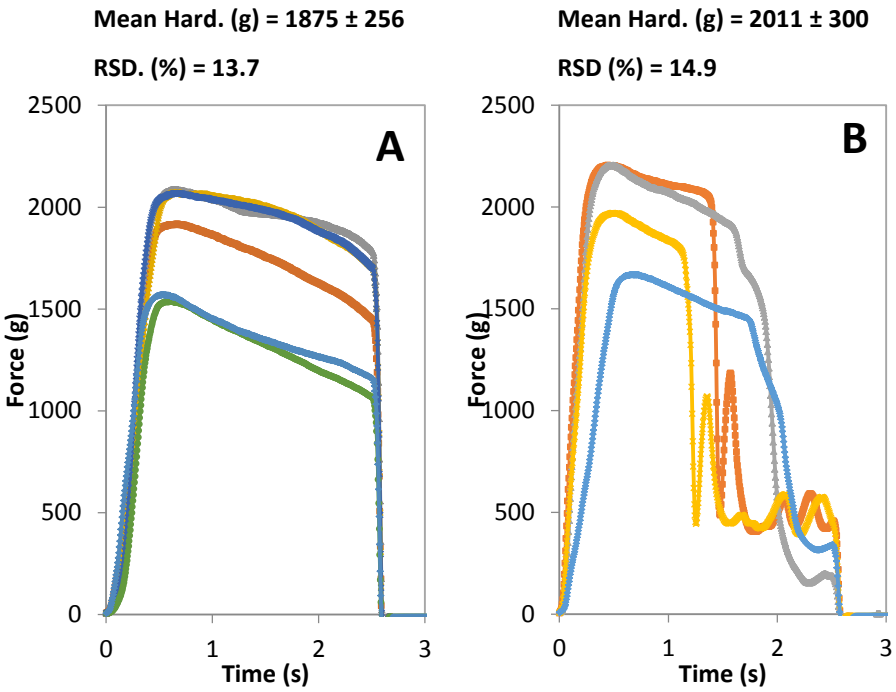

Figure 11: Force-time curves for the unbroken samples in (A) (6 replicates) and broken samples in (B) (4 replicates) for C-3, tested with Needle Method (section 2.4.1).

The charts illustrated in Figure 12 show the hardness data acquired with the cone penetrating on top (A) and the back (B) of the chocolate piece.

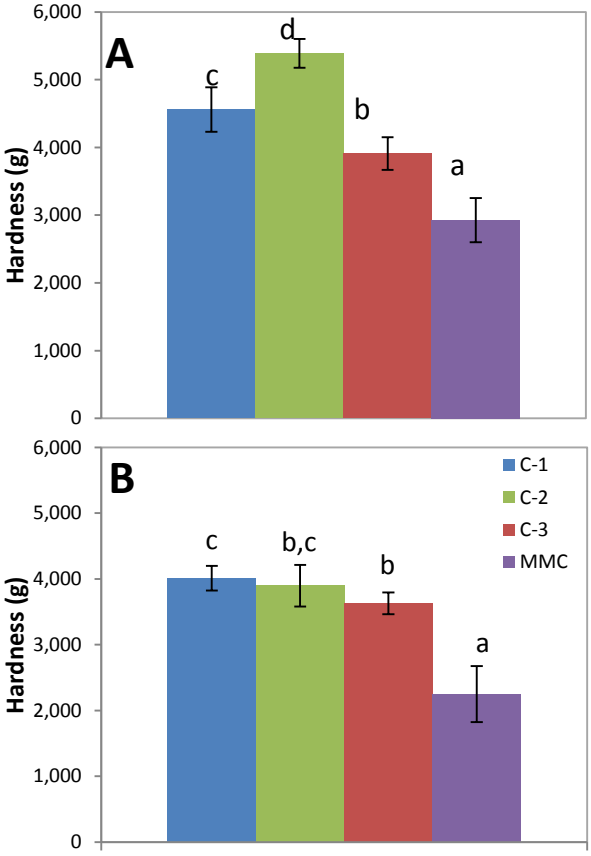

Figure 12: Hardness measured with the cone penetrating on top (A) and back (B) of chocolate piece. Samples with different letters indicate a significant difference ($p<0.05$) according to Tukey' HSD test. Legend is shown in (B)

Both cone probe methods gave higher values of hardness than the needle probe, showing probe dependence. Furthermore, chocolate piece orientation influenced the hardness values between the two cone probe methods. As shown in Figure 12, hardness values for the cone methods are generally higher when the cone penetrated on the top rather than on the back of the chocolate piece for each sample. In the method with cone penetrating on the top of the chocolate piece, the hardest sample was C-2, followed by C-1, C-3 and MMC, as in the needle method. As in the method

with cone penetrating on the top, hardness measured with cone penetrating on the back was higher for C-1 and C-2, despite C-2 showed a lower hardness value in the latter method as well as no significant difference between C-1 and C-2 was registered. Two important factors determining hardness of chocolate were reported as the fat content and particle size distribution (PSD) of the solids (Do *et al.*, 2007). PSD affects the structure of the chocolate; particles of smaller size have a higher total specific surface area, and higher level of interactions between them, which increases chocolate hardness. In contrast, particles of larger size have a smaller specific surface area and it results in fewer interconnections between them, they are more dispersed in the fat continuous phase and the chocolate hardness is reduced. The different hardness values of the chocolates are not related to the fat content since all four chocolates have a similar fat content. At the same time, although an inverse relationship between particles size and hardness was documented (Afoakwa *et al.*, 2008b; Do *et al.*, 2007), the four chocolates analysed in this study did not show that kind of trend. From the PSD data obtained from the manufacturer, C-3 and MMC showed lower values of D_{90} (90% finer) (see Table 7) compared to C-1 and C-2.

Table 7: Values of D_{90} (µm) for C-1, C-2, C-3 and MMC

	C-1	C-2	C-3	MMC
D_{90} (µm)	34.3	33.2	28.2	31.8

Another factor related to chocolate hardness is fat polymorphism, which affects the hardness of chocolate as density changes according to different fat polymorphic form. However, as reported in section 3.2, the four chocolates are characterised by the same polymorphic form, thus the differences in hardness between the four chocolates cannot depend to the fat crystal form.

The SFC is known to affect the hardness as higher SFC give harder chocolate (Full *et al.*, 1996). However, from the chocolates' SFC values shown in Table 6, the differences in hardness are not related to the different SFC of the four chocolates. Therefore, they must be related to other factors.

In milk chocolate, the amount of milk fat present in the continuous phase of the chocolate can vary according to the characteristics of the milk ingredient used in the manufacturing process, as the type of milk powder (Keogh *et al.*, 2002; Keogh *et al.*, 2003; Liang and Hartel, 2004). In particular, the increase of the milk fat in the continuous phase is related to the fact that this is no longer entirely protected by a native membrane called the milk fat globule membrane (Vignolles *et al.*, 2007). This type of fat has been called "free fat" by several authors. Higher amounts of this type of fat in milk powders reduce the ratio of the dispersed phase to the continuous fat phase in chocolate (Keogh *et al.*, 2004) and the amount of fat available for coating the solid particles would increase. Higher amount of "free fat" in the chocolate has been seen to reduce the hardness of chocolate samples (Keogh *et al.*, 2002; Liang and Hartel, 2004). Since the four chocolates show different hardness, it is possible to hypothesize that they contain different levels of milk fat in the continuous fat phase. In particular, the trend is always that C-1 and C-2 are harder than C-3 and MMC. Differences in the content of free fat in chocolates can be related to the different nature of the milk ingredient.

Both the needle method and the cone method with penetration on the top highlighted clear differences between the four chocolates, with higher levels of hardness for C-1 and C-2 compared to C-3 and MMC.

In order to compare the reproducibility of the three methods used, the values of RSD for each chocolate and each method are reported in Table 8. The results obtained with the needle method showed lower RSD, except for C-3, whose RSD value was higher compared to the cone methods. In the cone method with the probe penetrating on the back, MMC showed the highest standard deviation in general, which could depend upon the chocolate top surface shape, which was not plain and the stability of the chocolate piece during the analysis was reduced.

Table 8: RSD of the four chocolate for the three methods. The values are expressed in %.

	C-1	C-2	C-3	MMC
Needle method	4.65	2.59	13.03	4.37
Cone method top penetration	7.19	3.91	6.18	11.13
Cone method back penetration	4.63	8.11	4.54	18.90

In conclusion, the hardness of the chocolates may be determined by the amount of “free fat” rather than on particle size. Method with cone penetrating on the top showed similarities with the needle method regarding the trend between the samples, but the needle method gave frequently breakage of C-3. The method with cone penetrating on the back gave instead different trend compared to the other methods, so the method with cone penetrating on the top was considered the best for hardness measurements.

3.4 Meltdown behaviour

The melting behaviour of the chocolates was analysed by applying a constant load to cylindrical samples immersed in water at temperature above the chocolate melting temperature. The combined effect of temperature and constant load caused the melting and the consequent collapse of the cylinder and the results are shown as reduction of cylinder height vs time, referred to as a melting curve (see Figure 13).

Figure 13 shows the melting behaviour of the four chocolate samples, plotted as cylinder height over time (see section 2.5 for method).

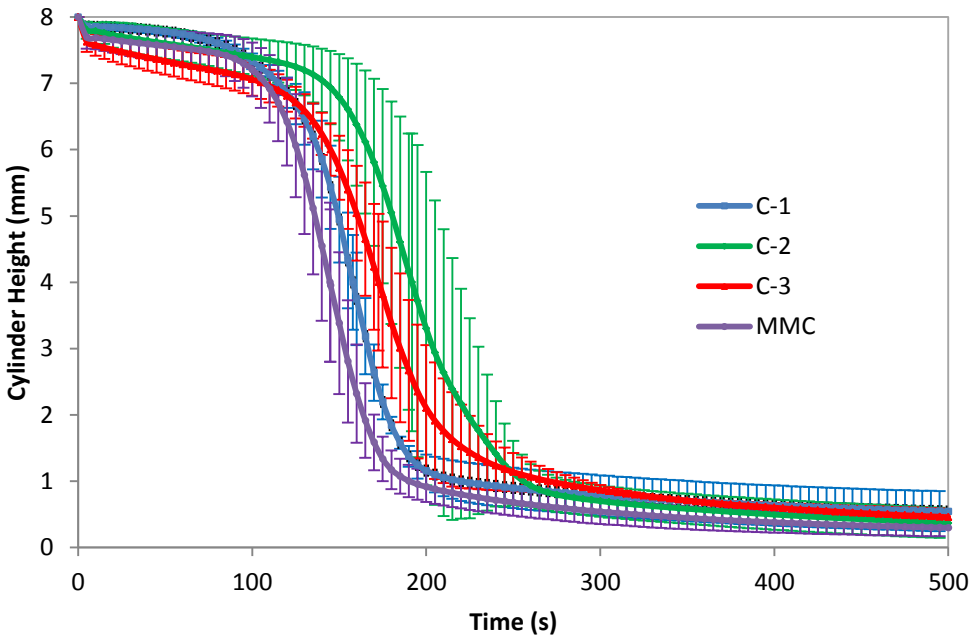

Figure 13: Meltdown behaviour of the four chocolate samples, average and standard deviation of three replicates measurements.

In the first part of the curves, where the slope is low, the cylinder still had mechanical resistance but a certain decrease in the cylinder height was observed and it might be due to the melting of the bottom and top surfaces of the cylinder. The heat transfer towards the centre of the cylinder caused instead its progressive melting and the consequent collapse, thus resulting in an increase in the probe lowering speed, which is represented as reduction

of cylinder height in time. Figure 14, Figure 15 and Table 9 show the mean values of *t-start*, collapse speed and $t_{50\%}$. The lack of time did not allow to run more replicates in order to improve the reproducibility.

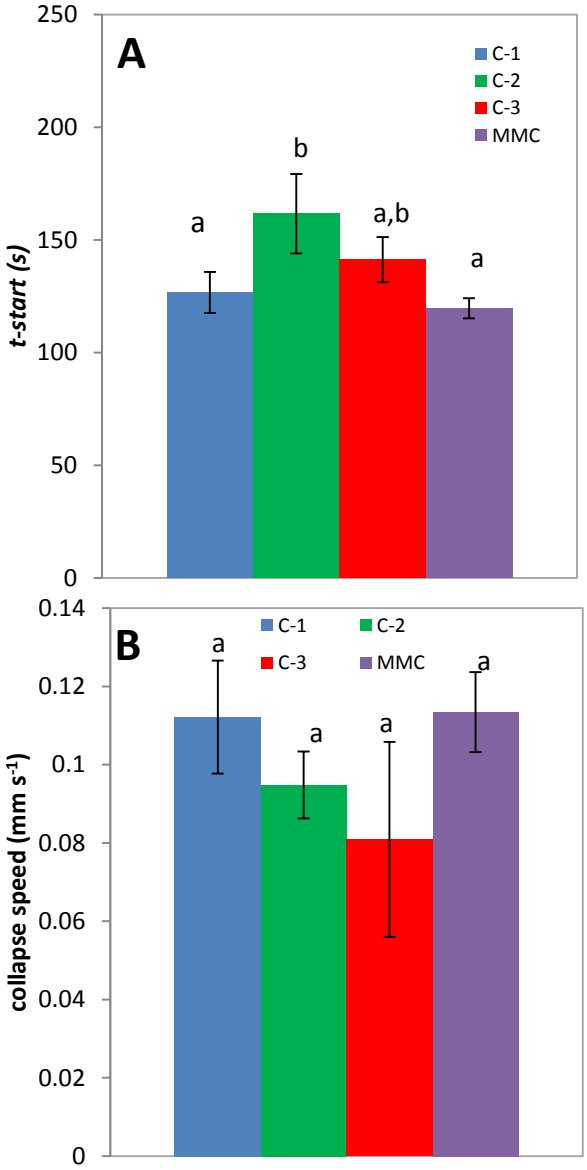

Figure 14: *t-start* (A), and collapse speed (B), for C-1, C-2, C-3 and MMC, as mean of 3 replicates. a-b means samples with different letter are significantly different ($p<0.05$) according to Tukey' HSD test.

As Figure 14 illustrates, C-2 had the highest *t-start*, followed by C-3 and then by C-1and MMC. The collapse speed data, instead, are not significantly

different but the trend appears to be that shorter *t-start* is related to higher collapse speed.

Table 9: Mean values and standard deviations of t-start, t50% and collapse speed.

	***t-start* (s)**	**Collapse speed (mm s^{-1})**	**$t_{50\%}$ (s)**
C-1	127±9	0.112±0.014	158±6
C-2	162±18	0.095±0.009	195±25
C-3	141±10	0.085±0.025	175±13
MMC	120±4	0.113±0.010	145±9

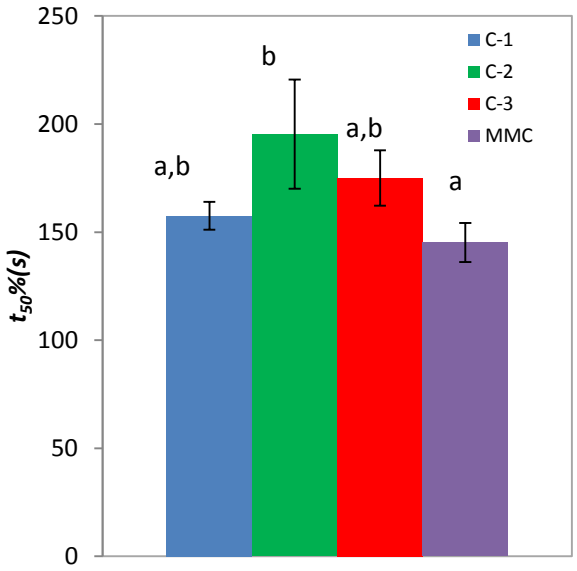

Figure 15: Values of $t_{50\%}$ (s) of the four chocolate samples, as mean of 3 replicates per sample. a-b means samples with different letter are significantly different (p<0.05) according to Tukey' HSD test.

In Figure 15 the values of $t_{50\%}$ of the four chocolate samples are shown as mean of 3 replicates per sample. The $t_{50\%}$ values ranking is in accordance

with the *t-start* ranking. As for *t-start,* C-2 showed the highest values of $t_{50\%}$, followed by C-3, C-1and MMC.

The influence of fat content in chocolate on *t-start* has been investigated by Do *et al.* (2007) who found direct correlation between the two parameters. Chocolates with higher fat content showed longer *t-start* compared to chocolates with lower fat content, and this was due to the lower thermal conductivity of fat compared to that of the chocolate solids. However, the differences observed between the chocolates in this study cannot be related to the amount of fat since the four chocolates have similar fat content and at the same time the melting properties analysed in section 3.2 are comparable between them, indicating the presence of one single polymorphic form, which is the same in the four chocolates. Besides, given the four chocolates did not show any statistical difference in collapse speed anyway, due to high standard deviation, the collapse speed values were not related to the different particle size in the four chocolates. The effect of particle size on collapse speed was evaluated by Do *et al.* (2007) and it was observed that higher solid particle size resulted in less particle aggregation and friction, and consequent higher collapse speed, but the effect of particle size on collapse speed lost importance in formulations containing 30% w/w of fat. Considering that the four chocolates in this study contain similar amounts of fat, this can explain why the collapse speed was not influenced by particle size.

Instead of considering one single factor as important in affecting chocolate meltdown behaviour, this appears to be related to a combination of factors which vary according to the formulation of the product, but further investigation is required to understand if single components such as the emulsifiers can have a role in the meltdown behaviour. This could be obtained by developing model chocolates to test the influence of type and amount of the different ingredients in the meltdown behaviour of the chocolate.

In order to evaluate the possible dissolution of the sugar from the chocolate cylinders in water, the volume of a C-1 chocolate cylinder was measured before the meltdown test and compared with the volume of the melted cylinder at the end of the test. In Table 10 the volume of the chocolate cylinder and that of the melted chocolate are shown.

Table 10: Volume (mm^3) of chocolate sample (C-1) before and after the meltdown test.

Chocolate Sample	Volume (mm^3)
Solid chocolate cylinder (before the test)	1069
Melted chocolate cylinder (end of the test)	660

As it is possible to infer from the table of above, the chocolate volume at the end of the meltdown test is lower than the initial volume, and this could be related to the dissolution of the sugar from the chocolate cylinder. The weight of the chocolate cylinder was 1.20 g and the amount of sugar calculated for the chocolate cylinder before the test was 0.672 g. Taking into account the hypothesis that the volume lost by the chocolate at the end of the test was represented by the sugar dissolved from the cylinder during the test, the amount of sugar lost in water was 0.650 g; therefore, almost all of the sugar must have been dissolved.

As shown by the curves obtained for the two completely greased chocolates (Figure 16), for both C-1and C-3 the differences in collapse speed (values in Table 11) between the two experiments are small, it is possible to hypothesize that the grease simply increases *t-start*, thus delaying the cylinder collapse. The grease would then act as a barrier to the heat transfer, and a longer time is needed to reach the centre of the chocolate cylinder. Once the collapse has started, the isolation effect of grease seems to be lost

due to lost integrity of the grease layer which would allow the water to get in contact with the chocolate. This observation is suggested by the fact that the final height of the chocolate cylinders in both the different experiments does not show important differences, especially in C-3 where the curves of the two experiments overlap in the time range between 300 and 500 s. Therefore it is possible to imagine that in the beginning the sugar dissolution concerns the area in contact with water, but once the structure starts collapsing, the shape of the cylinder modifies and water can penetrate in the chocolate through discontinuities in the structure.

Table 11: Values of collapse speed for C-1and C-3 for both experiments.

	C-1	**C-3**
Collapse speed (mm s^{-1})	0.112±0.014	0.081±0.025
Collapse speed – greased sample (mm s^{-1})	0.110	0.082

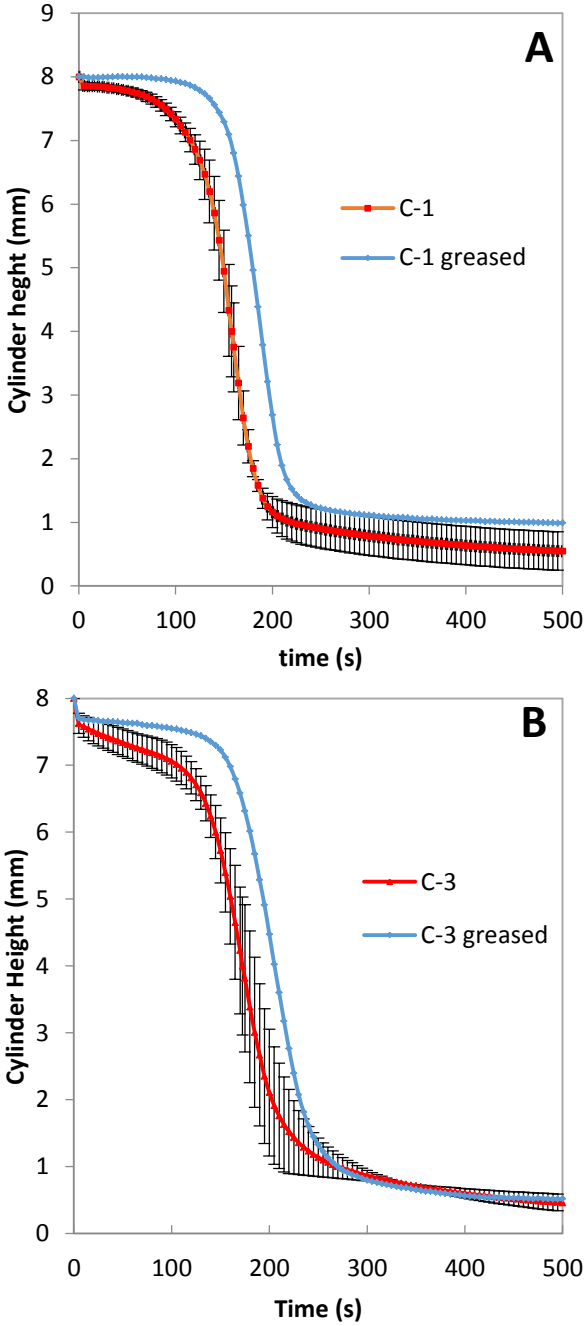

Figure 16: Meltdown curves of the completely and not completely greased chocolate samples for C-1 (A) and C-3 (B).

In Figure 17, the meltdown curve of the solid cocoa butter cylinder is shown.

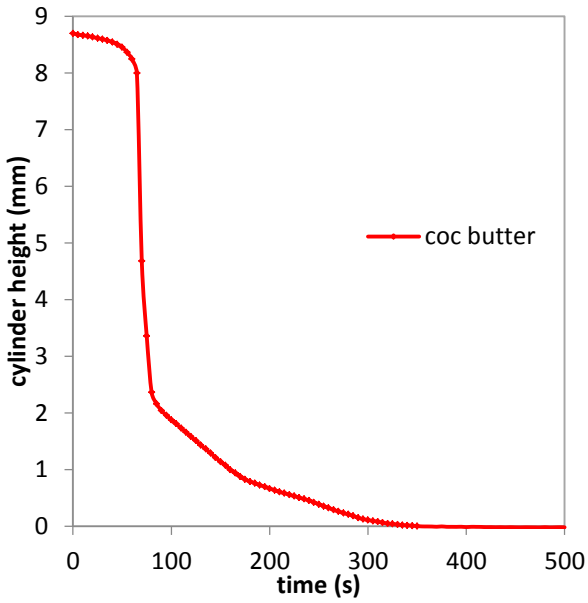

Figure 17: Meltdown curve of cocoa butter. No structure is maintained at already 350 s (Note: y-axis scale is 9 mm because the cocoa butter cylinder was slightly higher than chocolate cylinders).

According to (Do *et al.*, 2007), *t-start* was directly related to fat content in chocolate. Nevertheless, as it is possible to observe in the figure above, the meltdown curve of the cocoa butter cylinder reveals shorter *t-start* compared to the chocolate cylinders. It is however true that chocolate is a composite material and way the heat is transferred could differ compared to a system made only of fat such as cocoa butter.

Regarding the collapse speed, the cocoa butter cylinder showed higher value compared to the chocolate cylinder. The slope of the cocoa butter meltdown curve in the region of collapse is very high, due to the absence of solids in the cylinder. While in the chocolate cylinders the interactions between the undissolved solids allowed mechanical resistance to the collapse, in the cocoa butter cylinder, once the fat is melted, the collapse was almost immediate. At the same time the sample disintegrated and fat droplets were released in water (Figure 18).

Figure 18: Melted cocoa butter at the end of the test. Fat droplets dispersed in water are visible

This did not happen instead for the melted chocolate cylinders, in which the solids may have prevented the fat to be released in water. At the same time, as shown in Figure 19, not even the cocoa solids were dispersed in water, which remained clear, and the chocolate melted cylinder is clearly identifiable after the test and no disintegration occurred.

Figure 19: Melted chocolate at the end of the test. The water remained clear, indicating that no cocoa solids dispersed in the water

Although sugar dissolution in water is likely to take place, chemical determination of the sugar would be useful to quantify its solubilisation in water at the end of the test.

3.5 Rheology

3.5.1 Apparent viscosity and yield stress

The viscosity behaviour of the chocolate (see section 2.6.1 for method) samples, shown in Figure 20, indicates that all samples are shear thinning, which is typical of liquid chocolate. As shear rate increases, C-1and C-2 show higher viscosity compared to C-3 and MMC.

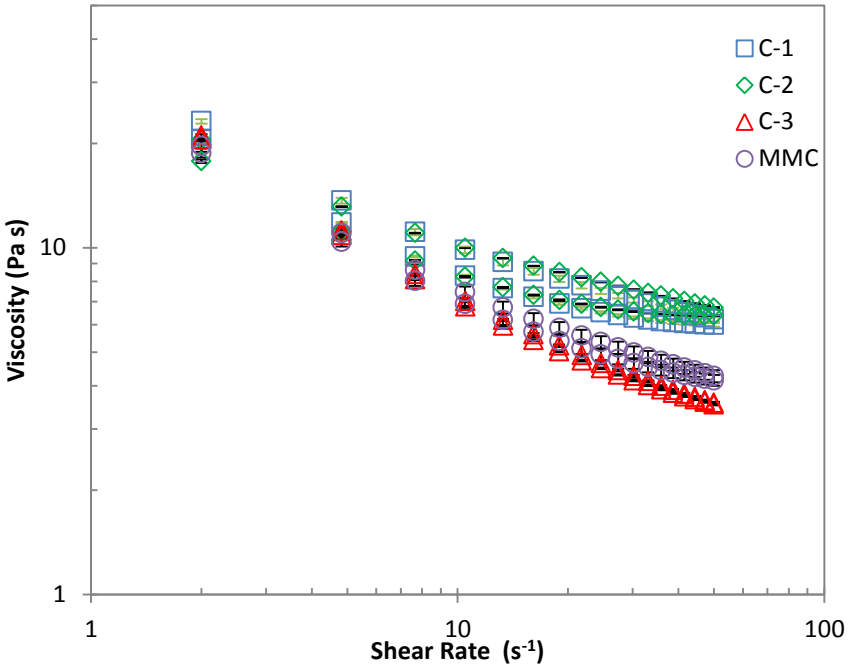

Figure 20: Apparent viscosity measured at 40°C for C-1, C-2, C-3 and MMC. The data are reported as average of 3 replicate measurements per sample and the standard deviation is within the size of the data point markers.

Figure 21 shows the values of η_{40} and YS5 for the four analysed chocolates as following the ICA method, as described in section 2.6.1.

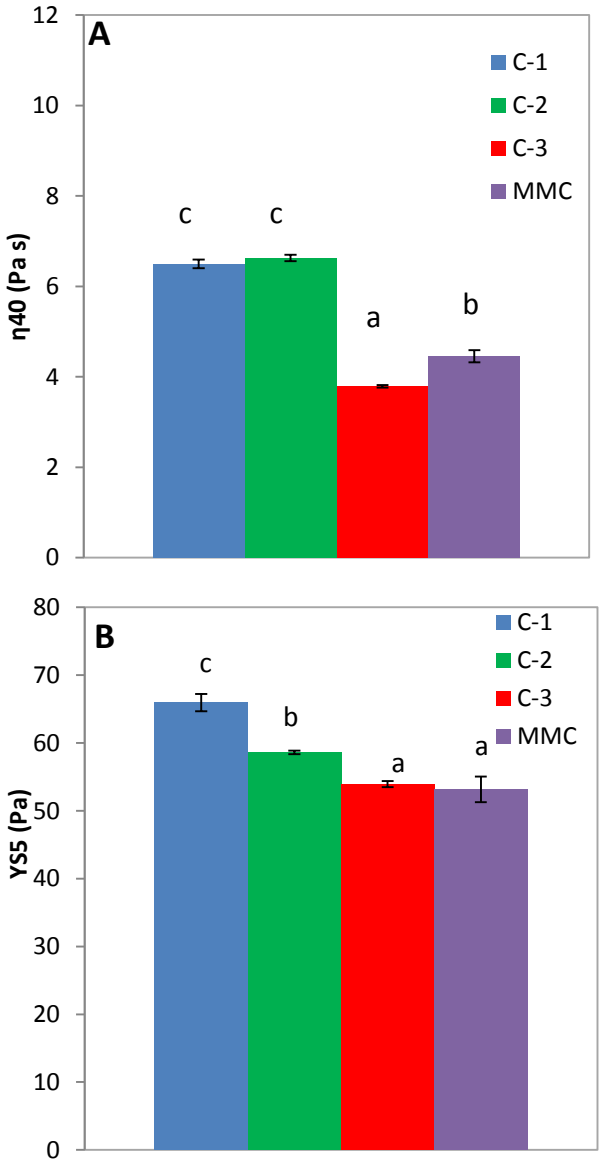

Figure 21: (A) Apparent viscosity at 40 s^{-1} – increasing shear rate ($\eta_{40,}$) of the four chocolates; (B) Yield stress at 5s^{-1} - increasing shear rate (YS5) of the four chocolates. a–c means samples with different letter are significantly different ($p<0.05$) according to Tukey' HSD test.

Table 12: Mean values and standard deviation of η40 and YS5 as shown in Figure 21.

	η_{40} (Pa s)	YS5 (Pa)
C-1	6.50±0.10	66.0.96±1.3
C-2	6.67±0.01	58.6±0.2
C-3	3.79±0.03	53.9±0.4
MMC	4.51±0.18	53.2±1.90

As for hardness and meltdown behaviour, chocolate rheological properties like viscosity and yield stress are affected by fat content and solid particle size (Do *et al.*, 2007; Ziegler and Hogg, 2009), type and quantity of emulsifiers. Fat content is the continuum phase in chocolate and it represents the liquid phase when chocolate is melted. The amount of fat determines the level of separation of the solid particles. Higher fat contents in chocolate reduces yield stress by reducing interactions between the solids; at the same time viscosity is lower because higher liquid content helps the flow.

Figure 20 shows that the differences in apparent viscosity between C-1and C-2 on one handside and C-3 and MMC on the other widen with increasing shear rate, highlighting higher viscosity for the first compared to the second two chocolates. As the fat content differs only by asmall amount between the samples, other parameters could affect the flow behaviour of the analysed chocolates. The manufacturing technology may determine the characteristics such as particle size distribution and milk fat content in the continuous phase of the final product.

Smaller particle size means higher specific surface area, so stronger interaction between solid particles, which creates a stronger network, with a more resistant structure (higher yield point) and higher resistance to flow (Do *et al.*, 2007; Servais *et al.*, 2004). As shown by the rheological results obtained on the four chocolates analysed, although particle size is important for chocolate viscosity, smaller particle size does not necessarily reflect in

higher viscosity of the molten chocolate, because the effect of other factors such as higher milk fat content in the continuous fat phase can overcome that of smaller particle size of the chocolate mix. The higher milk fat content in the fat continuous phase has been seen to depend on what is called “free fat” by several authors (see section 3.3). Lower values of viscosity and hardness (which depend on a combination of crystallized lipid phase and the solid dispersed phase - sugar crystals, cocoa solids and milk solids) have been seen to be correlated to higher levels of free fat in the chocolate (Liang and Hartel, 2004). The characteristics of the milk ingredient such as the type of milk powder (Campbell and Pavlasek, 1987; Keogh *et al.*, 2004; Liang and Hartel, 2004) may be related to different amounts of milk fat in the continuous fat phase of the chocolates. Since the viscosity values measured for MMC are closer to C-3 rather than to C-1 and C-2, it may be that one type of milk ingredient is used in C-1 and C-2, and a different type in C-3 and MMC. Higher amount of “free fat” would therefore explain the lower viscosity and the lower YS5 values of C-3 and MMC compared to C-1and C-2, despite the lower D_{90} shown by the first two chocolates..

3.5.2 Viscoelastic properties

In Figure 22, Figure 23 and Figure 24, the results of the oscillatory tests described in section 2.6.2 are shown summarized per method. In all three methods, characterised by the same strain amplitude (from 0.0012 to 10%) but with different pre-shear protocols (no shear, shear at 5 s^{-1} for 500 s and shear at 5 s^{-1} for 500 s plus 60 s rest in the first, second and third method respectively), all the samples show a trend for G' and G'' which can be divided into three characteristic regimes. When the strain amplitude is small, the G' module is larger than G'' and it is possible to observe the LVR, in which the viscoelastic moduli are independent from the strain amplitude; this corresponds to solid-like condition (van der Vaart *et al.*, 2013). As the strain amplitude increases, the viscoelastic modulus starts decreasing and the

system enters the nonlinear regime; here G'' becomes greater than G', and this can be interpreted as shear thinning behaviour.

The reduction of the G' modulus can be due to the breakage of the tri-dimensional structure of the sample, which occurs when the deformation amplitude exceeds a critical level, below which the melted chocolate behaves like a viscoelastic solid, while over that level the chocolate starts to flow (De Graef *et al.*, 2011). Over this limit, the structural network breaks and the sample is not able to completely recover its structure anymore. The higher the deformation is, the lower is G' because there is a further breakage of the material structure. Along with G', the increasing strain amplitude reduces the value of the G'', because the material particles tend to align with the shear flow and the resistance to flow is reduced (Wells, 2009).

Taking into account the two pre-shear step methods, it is possible to observe that while C-1, C-2 and MMC viscoelastic curves partially overlap, C-3 has a different behaviour. C-3, in fact, shows higher values of G' and G'' at both the shortest and widest strain amplitudes, and the lowest G'' at strain amplitudes between 0.03 add 1%. The highest values of G' in the LVR are shown by C-3 and can be related to the fact that C-3 has the smallest particle size among the four chocolates, reflecting a higher specific surface area and more interconnections between the particles. MMC has the second smallest particle size value and it registered the second highest G' in the LVR for the method with 500 s pre-shear step, whilst no detectable differences are seen for the other two methods. Although C-3 shows the highest G' in the LVR, the lower values of viscosity reported for C-3 (as well as MMC, see section 3.5.1) compared to C-1 and C-2, might depend more on the effect of free fat content rather than particle size.

The differences in G' between C-3 and the other chocolates are less detectable in the no pre-shear step method, furthermore the no pre-shear method shows higher standard deviation compared to the other methods, because the lack of pre-shear step results in a less homogeneous system.

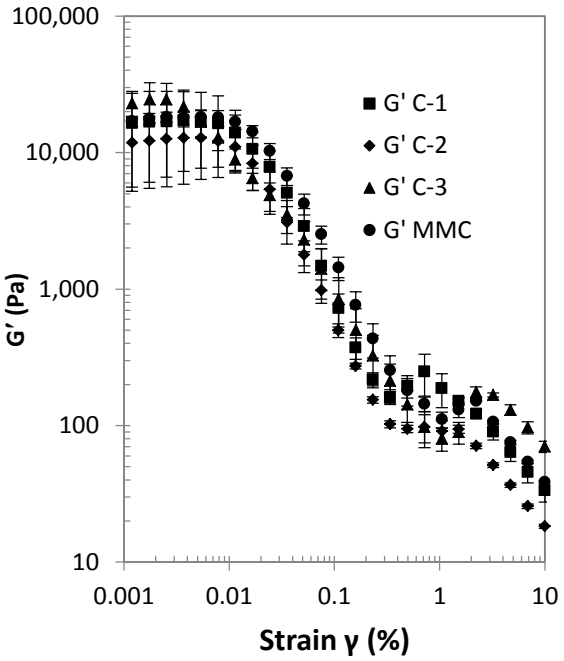

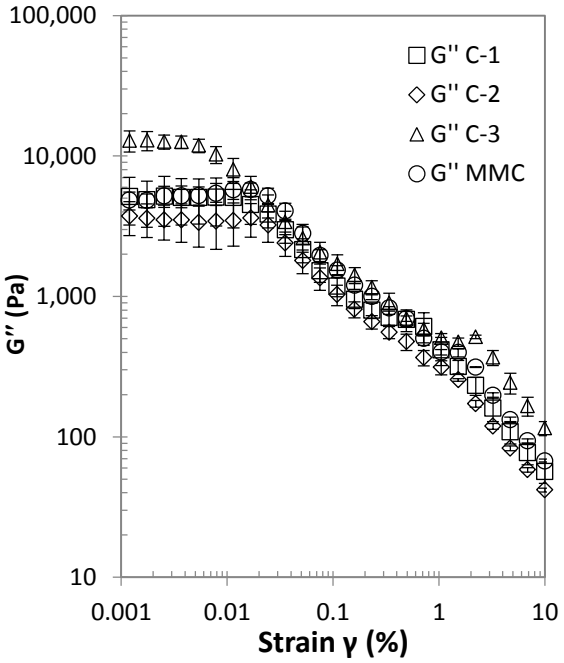

Figure 22: G' and G'' moduli as function of strain for the 4 chocolate samples, method with no pre-shear protocol applied.

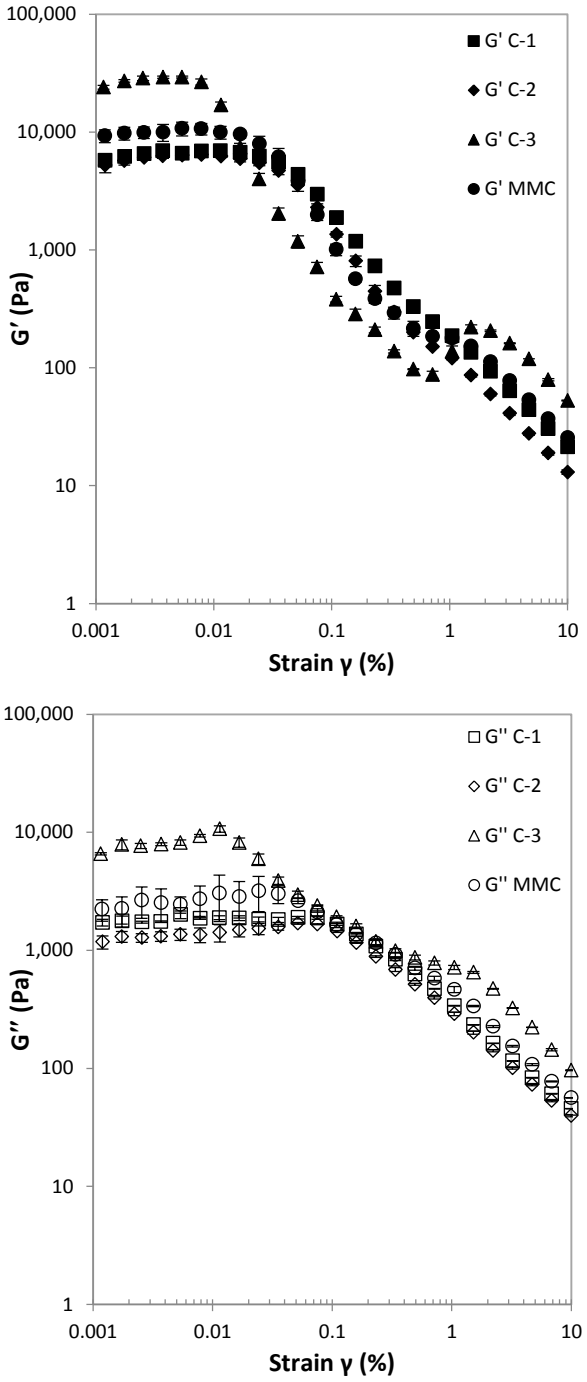

Figure 23: G' and G'' moduli as a function of strain γ for the 4 chocolate samples. 500 s pre-shear protocol at 5 s^{-1} was applied before strain sweep.

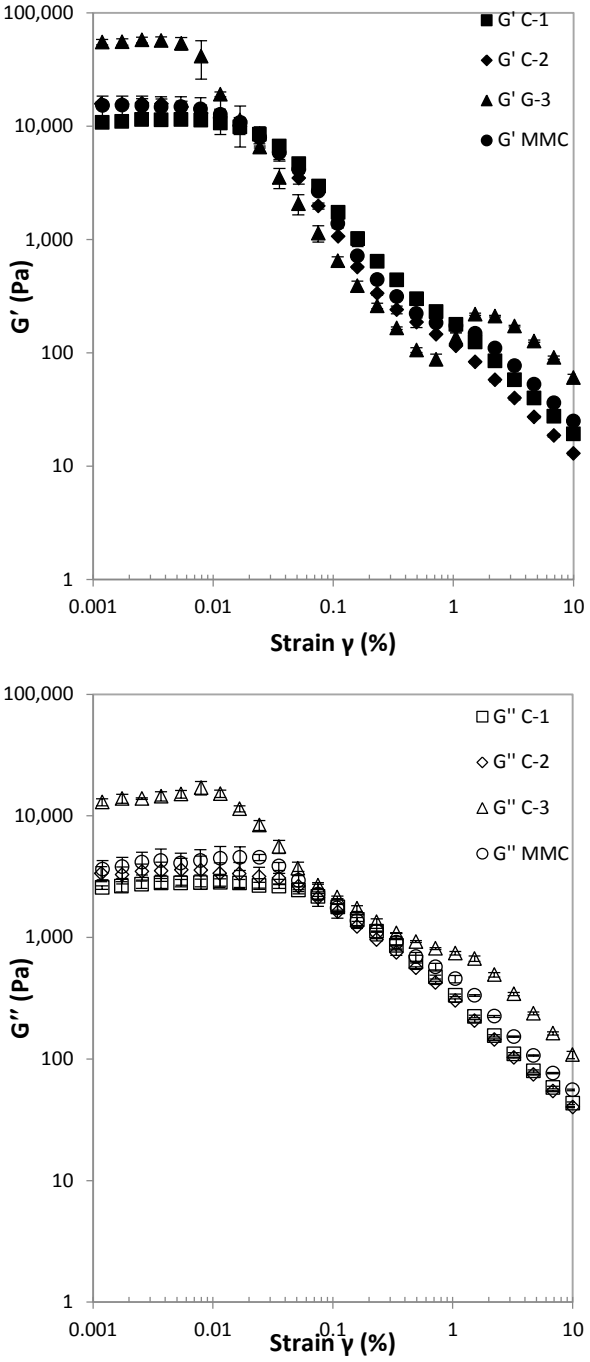

Figure 24: G' and G'' moduli as a function of strain for the 4 chocolate samples, 500 s pre-shear protocol at 5 s^{-1} followed by a 60 s period of rest (zero shear), was applied before strain sweep.

In Figure 25-Figure 28, the G' and G'' moduli for the four chocolate samples are depicted summarized per sample. In each figure, the results relative to all three methods applied are compared for each sample. All the three methods

show values of G' and G'' of the same order of magnitude for all the chocolates. The chocolates viscoelastic behaviour shows the highest differences between the methods at low strain amplitudes, where the LVR is found. At higher strain amplitudes, the values between the different methods generally overlap, except for C-1 and C-2, which show lower values of G' modulus with no pre-shear method, at strains between 0.04% and 0.8%. The lowest G' and G'' in the LVR are found in the pre-shear with no-rest step method for all the chocolates. The use of a pre-shear step will break the structural network which reduces the degree of interconnection between the solid particles and the resistance to the flow is reduced, thus reducing the chocolate viscoelastic modulus. G' and G'' in the pre-shear with rest step method are instead higher and more similar to the values found with no pre-shear method. The rest period allows the structure, broken by the pre-shear step, to recover, restoring the interactions between the solid particles.

All the samples show lower G' when the pre-shear with no rest step is applied, except C-3, whose maximum storage modulus values found with this method are similar to those found with no pre-shear method, whilst higher G' modulus is found for the method with shear and rest step. C-3, in particular, shows shorter LVR in the no pre-shear method (γ about 0.003%), especially for G', compared to the pre-shear methods, which have similar LVR extension (γ around 0.008%). The solid state seems to resist to higher strains when the pre-shear step is applied.

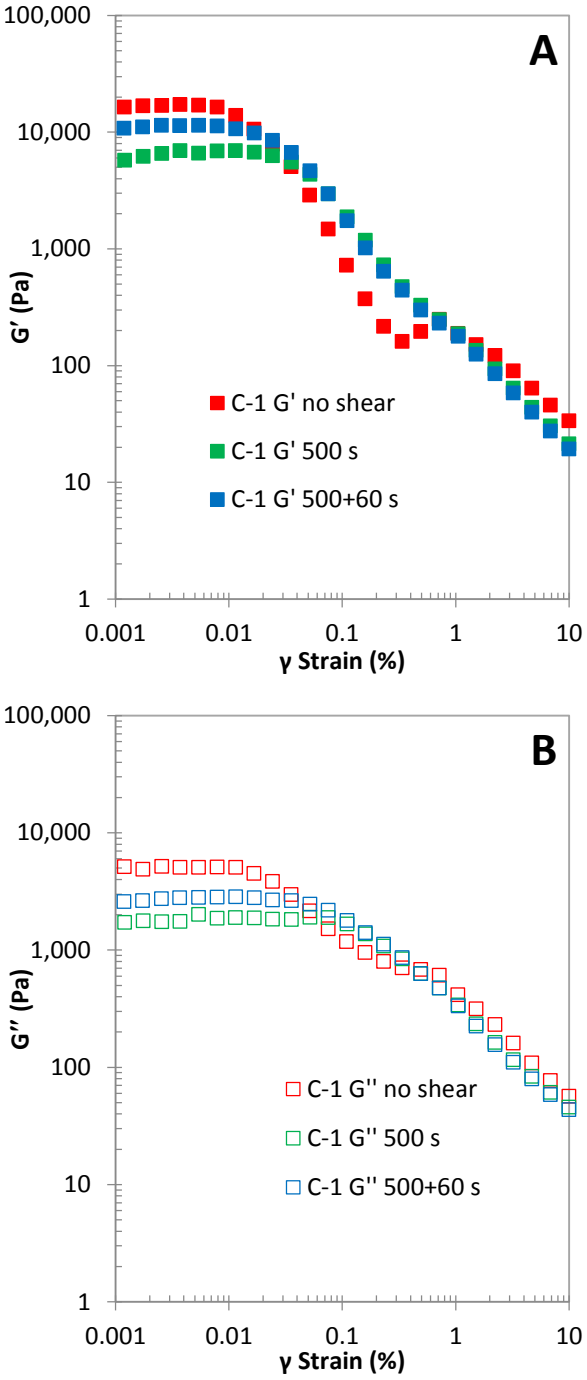

Figure 25: G' (A) and G'' (B) moduli as a function of strain for C-1. The three methods used are compared; in order to better visualize the data, error bars were omitted.

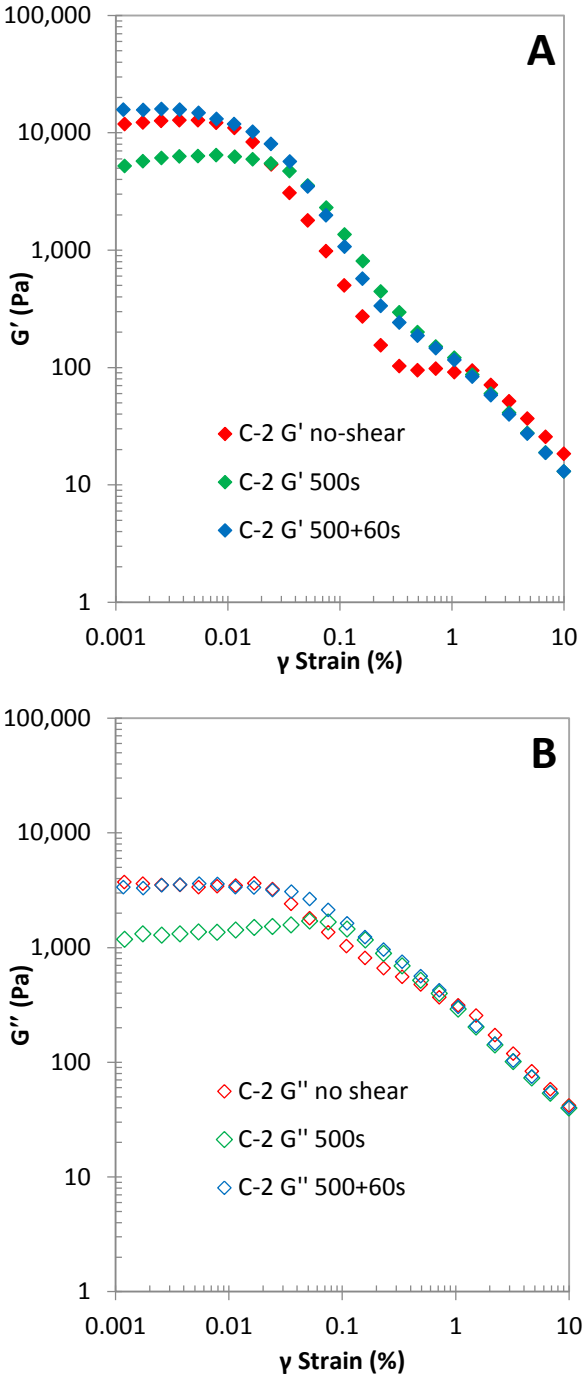

Figure 26: G' (A) and G'' (B) moduli as a function of strain for C-2. The three methods used are compared; in order to better visualize the data, error bars were omitted.

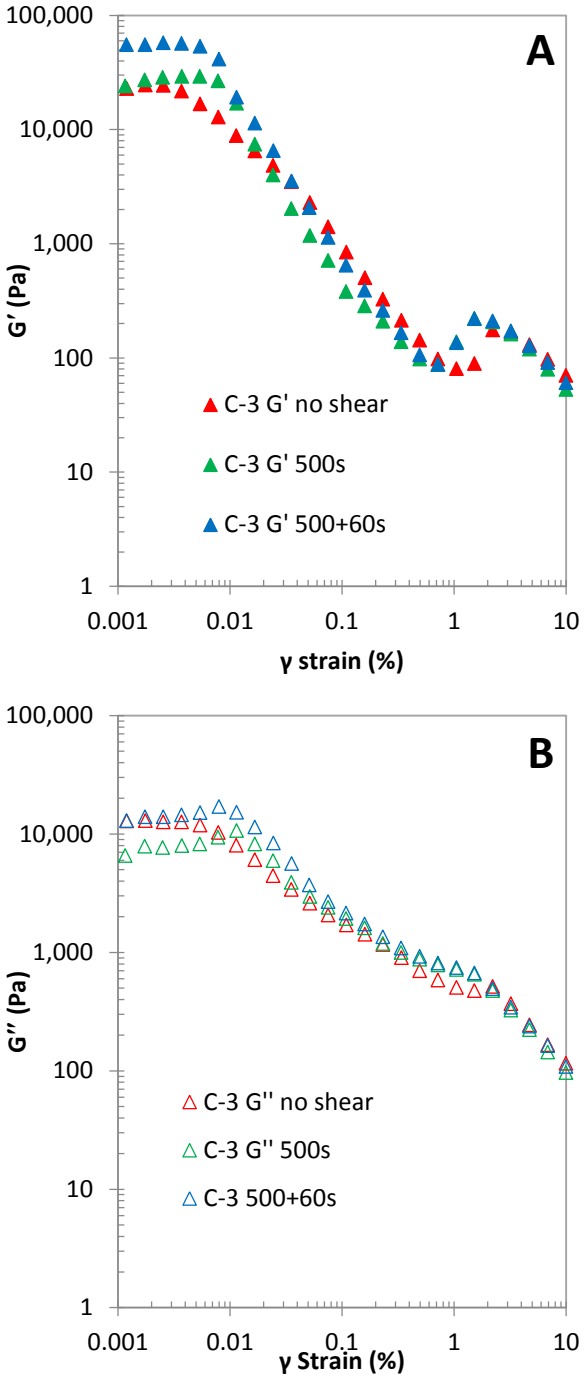

Figure 27: G' (A) and G'' (B) moduli as a function of strain for C-3. The three methods used are compared; in order to better visualize the data, error bars were omitted.

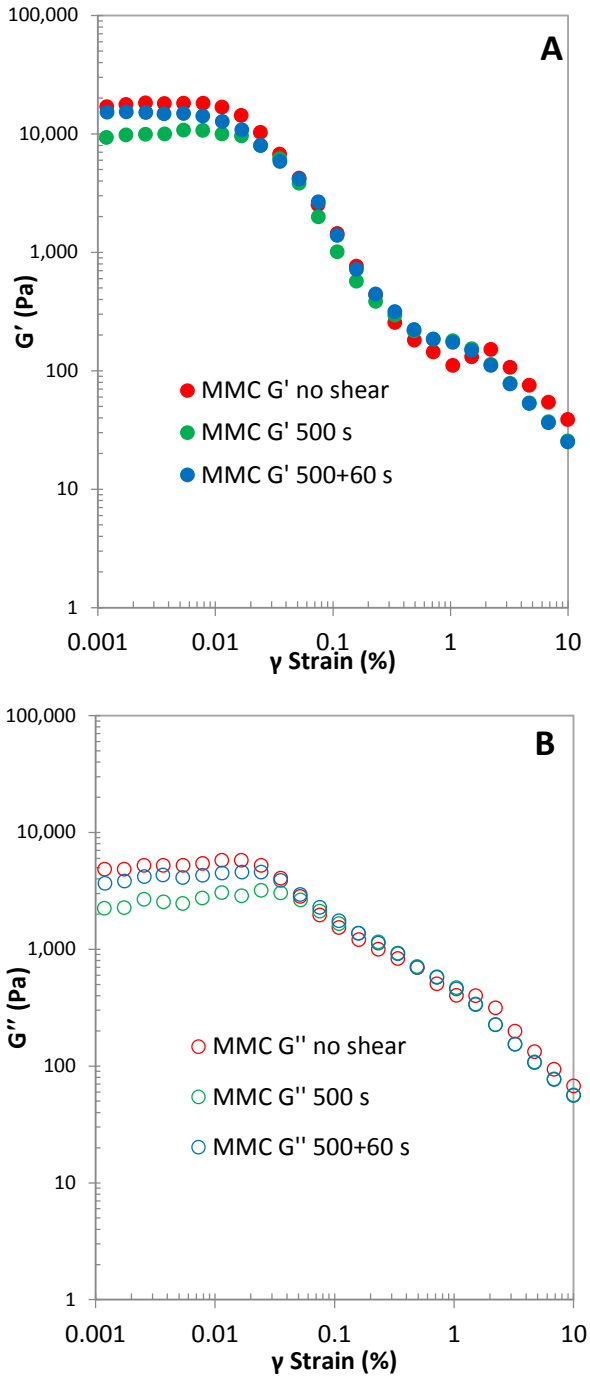

Figure 28: G' (A) and G'' (B) moduli as a function of strain for MMC. The three methods used are compared; in order to better visualize the data, error bars were omitted.

According to De Graef *et al.* (2011), oscillatory rheology can be used as an alternative to flow curve to determine the yield stress in chocolate. In Figure 29, the values of the G′ modulus are plotted as a function of the

correspondent shear (oscillatory) stress values, for the four chocolates. Since no important differences were found between the three methods, only the data relative to the pre-shear without rest step method are shown, whose pre-shear step corresponds to that used in steady shear rheology measurements. The stress value which corresponds to the decrease of G', that is the end of LVR, is considered as the yield stress. The yield stress values (YS5) found with steady shear rheology are higher compared to those in oscillatory rheology, furthermore the YS5 values of C-3 and MMC are similar between them and lower than those of C-1 and C-2. The yield stress values found with oscillatory rheology measurements do not show instead difference between the chocolates, as shown in Figure 29. However, while the yield stress in oscillatory rheology is related to the breakage of the tri-dimensional network in the chocolate, which happens at the end of the LVR, the YS5 value measured with steady shear rheology reflects the yield stress in flowing chocolate, therefore the methods reflect two different material conditions. At the same time, increasing the oscillation frequency to higher values can enhance the differences in the yield value between the chocolates. Further analysis at higher frequencies of oscillation could thus provide more information about differences in the yield stress between the chocolates.

In Figure 29, C-3 shows the highest G' values; this may be a result of the smaller particle size distribution of C-3 compared to the other chocolates. Higher interaction degree between the particles could cause the elastic modulus to increase. At the end of the LVR, C-3 shows a sudden drop of G' compared to the other samples; this higher decrease in G' modulus could explain the lower viscosity that C-3 has in comparison to C-1 and C-2.

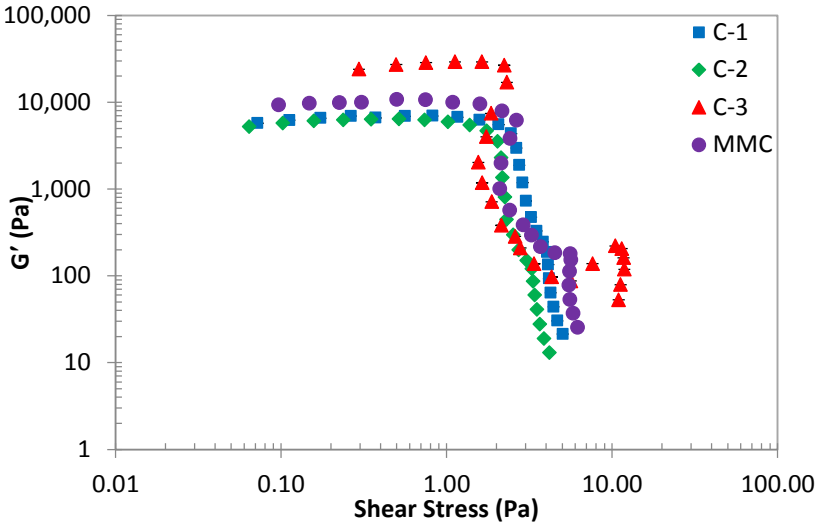

Figure 29: G' modulus as a function of shear stress for C-1, C-2, C-3 and MMC, measured with 500s at 5 s^{-1} pre-shear and no rest step method. The yield point can be determined as the shear stress value at which G' reduces, at the end of the LVR.

3.5.3 Information supplied by rheological analysis

- The different values of viscosity shown by the chocolates can be directly related to different amounts of milk fat in the continuous fat phase, which may depend on the different nature of the milk ingredient.
- The higher G' shown by C-3 compared to the other chocolates may depend on its D_{90}, which is the smallest among the four chocolates. The yield stress measured in steady shear rheology (YS5) for C-3 and MMC is lower than for C-1and C-2, whilst the chocolates reported comparable yield stress values when measured with oscillatory rheology. The yield stress in oscillatory rheology is related to the breakage of the tri-dimensional network in the chocolate, and it reflects the end of the solid-like condition. The YS5 value measured with steady shear rheology reflects the yield stress in flowing chocolate, therefore the methods reflect two different material conditions.

3.6 Friction properties

The results related to friction behaviour tests described in section 2.7 are reported as follows. In section 3.6.1 and 3.6.2, the results of the PU friction surfaces tests and the chocolate friction behaviour, performed on PU surfaces, are respectively described. The results of the PDMS surface tests are instead described in section 3.6.3, while in sections 3.6.4 and 3.6.5 the two friction tests on chocolate performed with PDMS surfaces are reported.

3.6.1 PU friction surfaces

The friction properties of a PU friction surface set used in this research were tested before and in between tribological measurements on chocolate. The measurements with sunflower oil were conducted to evaluate the consistent performance of the surfaces used for analysis of the friction properties of chocolate. The friction properties of this set of surfaces acquired at increasing sliding speed following conditioning step are shown in Figure 30A (run 1) and the results of the repeated measurements (run 2) are reported in Figure 30B.

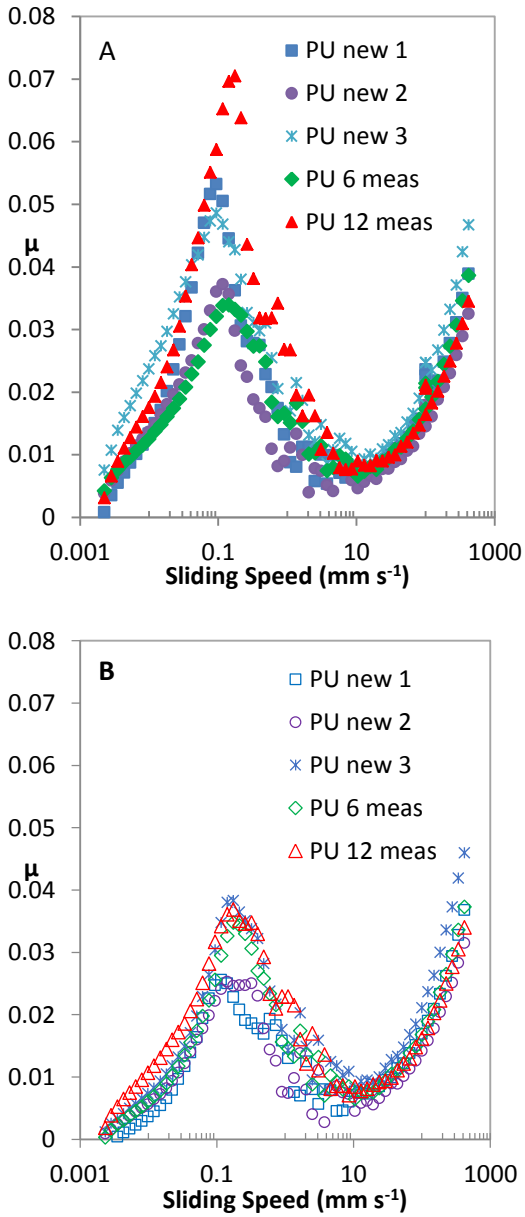

Figure 30: Friction behaviour of sunflower oil measured with PU surface set. The results in (A) correspond to the first measurement (run 1) following conditioning, whilst the results in B correspond to the repeated measurement (run 2) immediately following run 1. Three test replicates were performed before commencing the tribological measurements on chocolate (PU new 1, PU new 2, PU new 3), while the following tests with sunflower oil were performed in single replicate, after six (PU 6 meas) and 12 (PU 12 meas) chocolate tribological measurements. Surfaces were cleaned after each measurement. Conditioning speed was 100 mm s^{-1} and applied normal force throughout analysis was 0.5 N.

The values of friction coefficient depicted in Figure 30 show random but small variability. Considering that sunflower oil was used as reference material, this reflects the variability of the method, which is well below the μ values of the four chocolates. In order to compare the results of chocolates and sunflower oil, in Figure 36 the friction curve of sunflower oil (presented as average of 5 replicates) is shown together with the friction curves of the four chocolates. The maximum variability of μ in sunflower oil, which was found in the mixed regime at 0.1 mm s^{-1} sliding speed, is about 0.02, much smaller than the μ values found in the correspondent mixed regime for chocolate measurements. The variability of the friction results with sunflower oil is even smaller in run 2.

Preconditioning at sliding speed below the hydrodynamic region while applying the higher level of normal force was not analysed, this in hindsight can be regarded as an oversight and it will be considered in future measurements.

The friction curves related to the surface test at 3 N are shown in Figure 31. The results on the tests at 3 N reveal the same friction behaviour of those at 0.5 N, with good reproducibility even after the tests on chocolate.

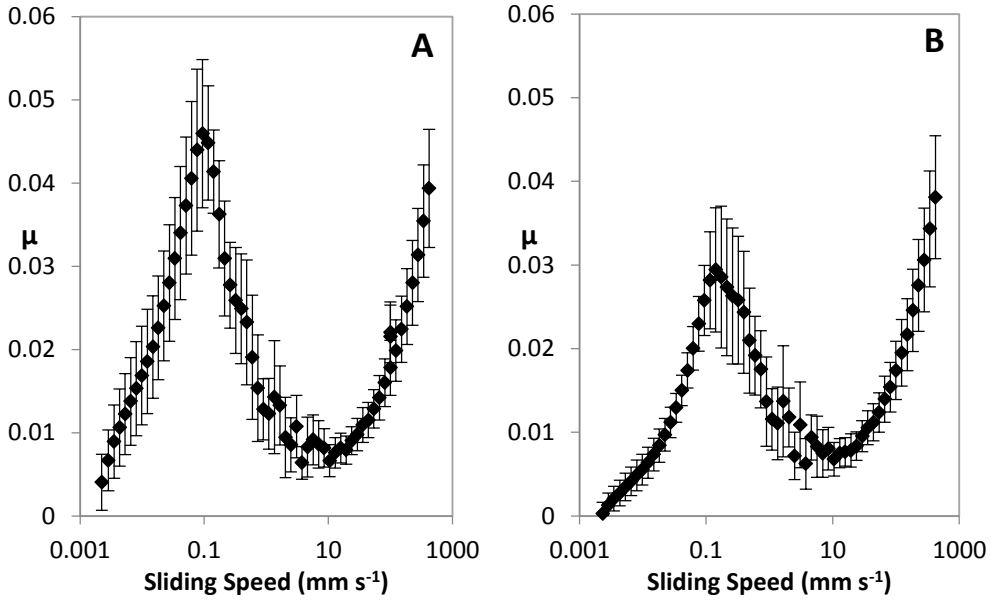

Figure 31: Friction behaviour of sunflower oil measured with PU surface set. The results in (A) correspond to the first measurement (run 1) following conditioning, whilst the results in B correspond to the repeated measurement (run 2) immediately following run 1. Conditioning speed was 100 mm s^{-1} and applied normal force throughout analysis was 3 N. Surfaces were cleaned after each measurement. The test was conducted in triplicate after having completed the friction test on the four chocolates.

3.6.2 Frictional properties of the chocolate samples - PU surface sets

The Stribeck curves for the four chocolates analysed in this study are shown in Figure 32-Figure 35. Part A in each figure refers to the initial measurement (run 1) and part B in each figure shows the results of the repeated measurement (run 2) on the same chocolate.

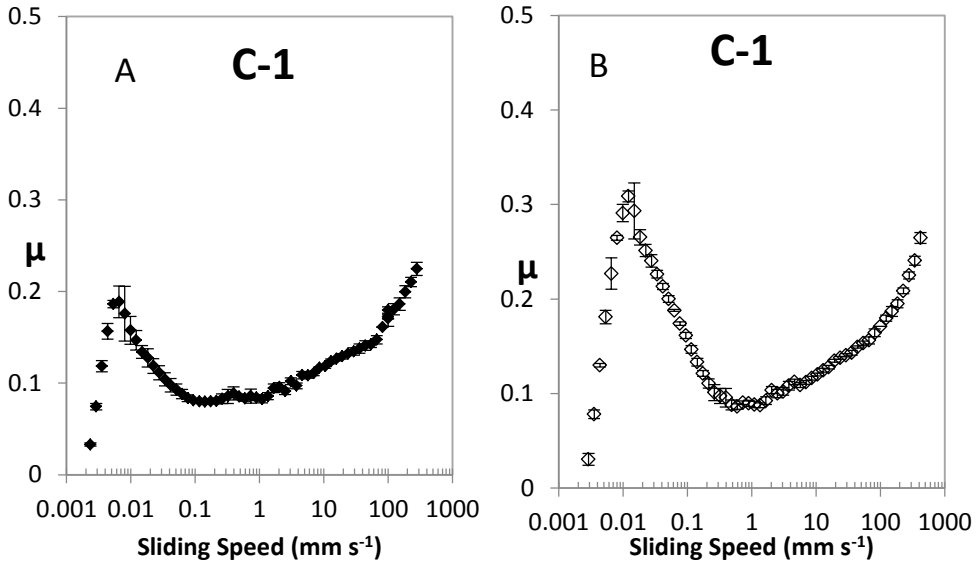

Figure 32: Friction behaviour of C-1at 37°C and 3 N applied normal force. (A) shows the results of the first measurement following conditioning at 100 mm s^{-1} and (B) shows the results of the repeated measurement (run 2) immediately started after run 1 omitting the conditioning step. Sliding speed was increased from 0.001 to 420 mm s^{-1} in 240 seconds.

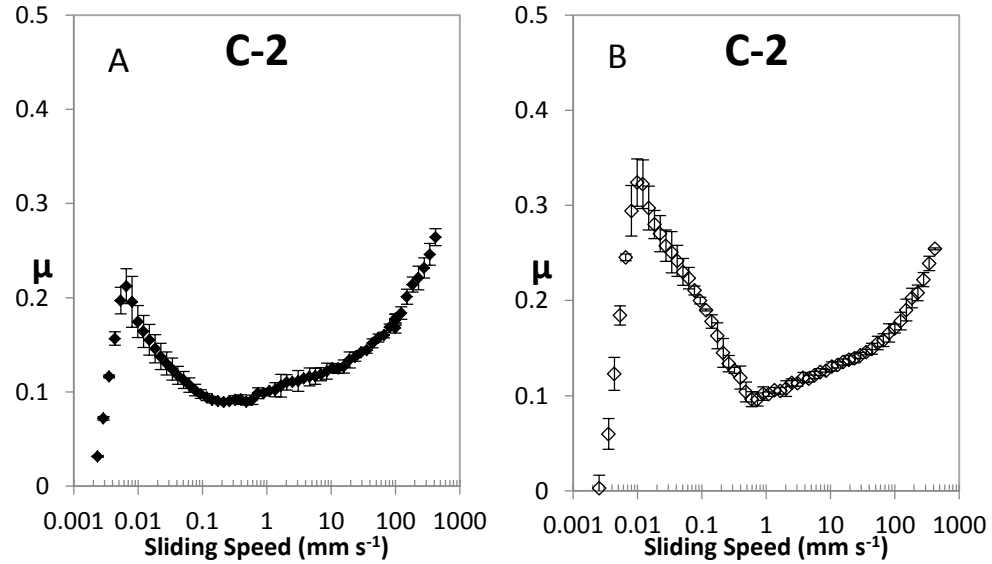

Figure 33: Friction behaviour of C-2 at 37°C and 3 N applied normal force. (A) shows the results of the first measurement following conditioning at 100 mm s^{-1} and (B) shows the results of the repeat measurement (run 2) immediately started after run 1 omitting the conditioning step. Sliding speed was increased from 0.001 to 420 mm s^{-1} in 240 seconds.

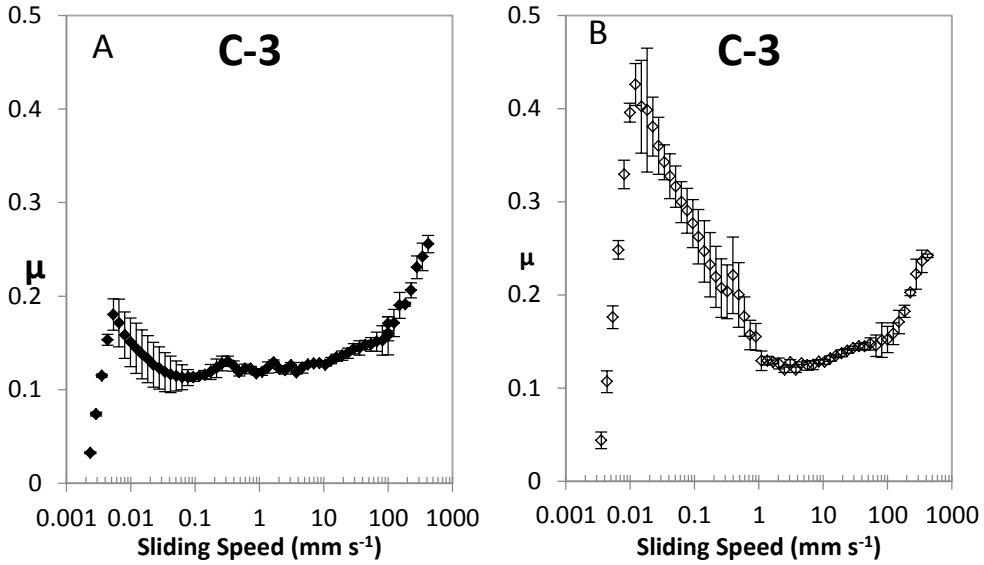

Figure 34: Friction behaviour of C-3 37°C and 3 N applied normal force. (A) shows the results of the first measurement following conditioning at 100 mm s^{-1} and (B) shows the results of the repeat measurement (run 2) immediately started after run 1 omitting the conditioning step. Sliding speed was increased from 0.001 to 420 mm s^{-1} in 240 seconds.

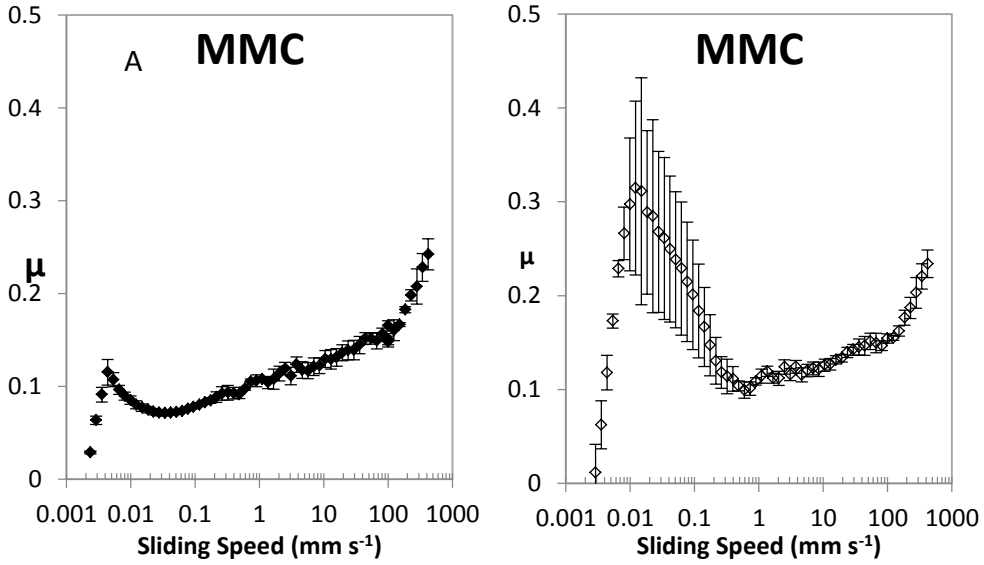

Figure 35: Friction behaviour of MMC at 37°C and 3 N applied normal force. (A) shows the results of the first measurement following conditioning at 100 mm s^{-1} and (B) shows the results of the repeat measurement (run 2) immediately started after run 1 omitting the conditioning step. Sliding speed was increased from 0.001 to 420 mm s^{-1} in 240 seconds.

The results of the first measurement following conditioning and the second measurement immediately following the first measurement are different for all four chocolates. This result is not surprising since the sliding speed applied during conditioning was lower than the maximum sliding speed applied in the actual measurement. For all four chocolates the conditioning sliding speed of 100 mm s^{-1} fell into the hydrodynamic regime. It appears that there is a slight kink in all four graphs showing the results of run 1 which may be related to the choice of 100 mm s^{-1} as conditioning sliding speed; it is surprising that this kink is also apparent in the results of run 2. It can be hypothesised that choosing the highest speed applied in the run as sliding speed would lead to overlapping results of run 1 and run 2. On the other hand, the effect of omitting the conditioning step can be observed in the third of the three methods adopted, where run 1 did not follow any conditioning step. The results of run 1 would then reflect the entrainment of chocolate between the two friction surfaces potentially providing insight into different wetting behaviour. The results of run 2 are most likely dominated by the properties of the sugar, cocoa or milk particles in chocolate. They entrain into the gap between the two sliding surfaces and may "stick" to the surfaces when the measurement is stopped following either conditioning or run 1, influencing the results in the boundary regime or rather the mixed regime. A boundary regime cannot be identified in the Stribeck curves acquired; this observation has already been made by Carvalho-da-Silva *et al.* (2013). Instead, a sudden increase of the friction coefficient at low sliding speeds is observed. This kind of behaviour was explained by Carvalho-da-Silva *et al.* (2013) as a result of an elastic response below a critical friction force. To facilitate comparison between the four chocolates, the results have been combined in Figure 36.

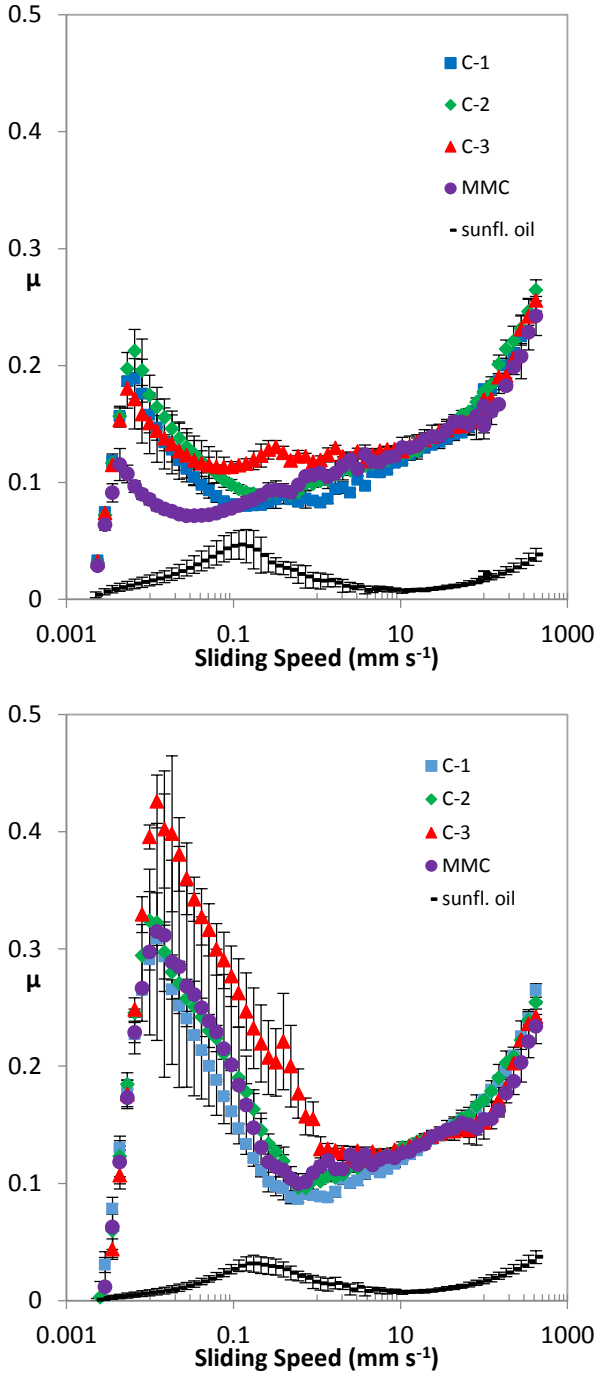

Figure 36: Combined presentation of the results shown in Figure 32, Figure 33, Figure 34 and Figure 35. The friction curve obtained with sunflower oil is also shown, as average of five replicates.

Of the four chocolates, MMC shows the lowest friction coefficient in the mixed and elasto-hydrodynamic regime comparing the samples based on the results of run 1. While at the onset of the mixed regime the data for the

other three chocolate samples overlap, C-3 shows an upward trend at sliding speed between 0.1 and 1 mm s^{-1}. At sliding speeds above 1 mm s^{-1} the results coincide, this is also the case for the results of run 2. Lee *et al.* (2002) already reported that the differences in friction behaviour between chocolate samples tended to reduce at higher speeds (over 1 mm s^{-1}). In run 2, C-3 does not show this discontinuity, except for a slight transitory increase at about 0.5 mm s^{-1}; here it shows throughout higher friction coefficients than the other three samples which appear not distinguishable in this test.

3.6.3 PDMS friction surfaces

One set of PDMS friction surfaces was tested with liquid cocoa butter as reference material before and in between tribological measurements on chocolate, in order to evaluate the consistent performance of the surfaces used for analysis of the friction properties of chocolate. The tests were performed using the same method applied to sunflower oil on PU surfaces. The results of the friction tests are shown in Figure 37 (A) (run 1) and Figure 37 (B) (run 2).

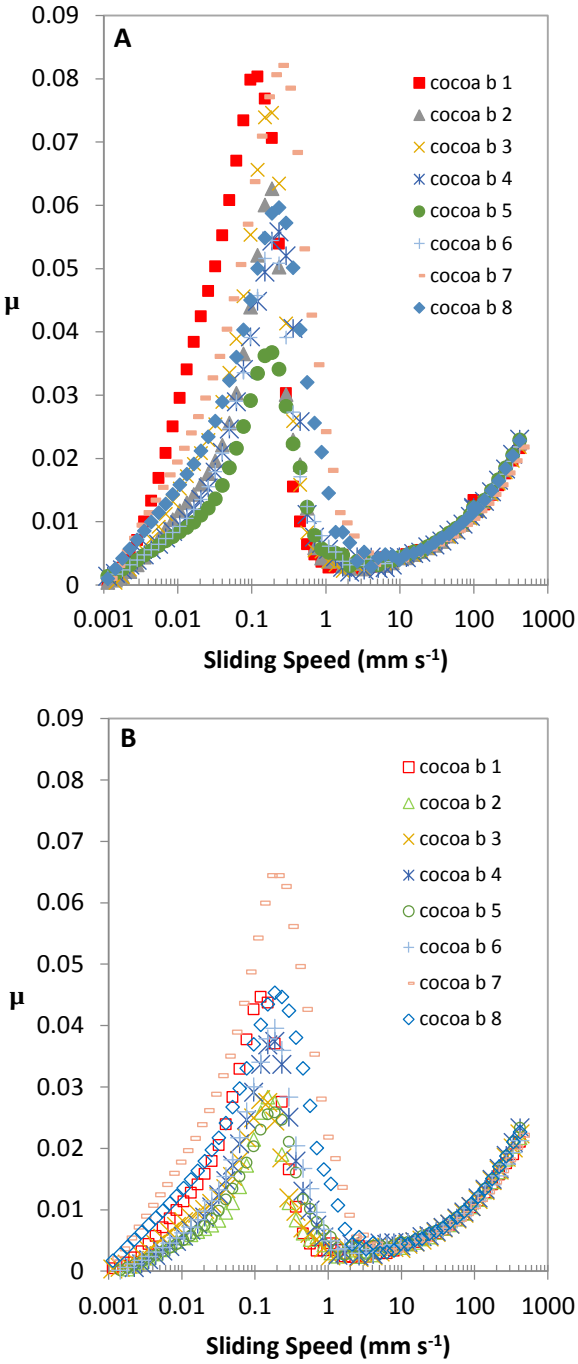

Figure 37: Friction behaviour of cocoa butter measured with PDMS surface. The new surface was tested three times before starting using it for chocolate tribological measurements. Surfaces were cleaned after each measurement. Conditioning and applied normal force throughout analysis was 100 mm s^{-1} and 3 N respectively. Two consecutive test runs were performed for chocolate and the results of run 1 and run 2 are depicted in (A) and (B), respectively.

The measurements with cocoa butter were conducted to evaluate the consistent performance of the surfaces used for analysis of the friction properties of chocolate. As shown in Figure 37, the friction coefficient in run 1 is higher than in run 2, in the sliding speed range from 0.001 up to 10 mm s^{-1}, with peak values generally between 0.06 and 0.08 in run 1, and between 0.03 and 0.05 in run 2. The lower friction coefficient found in run 2 might depend on the fat adsorption on PDMS surface, acting as lubrication layer. As for sunflower oil (see section 3.6.1), the μ variability of the surface test with cocoa butter is far below the μ values found on chocolate for the methods of sections 3.6.4 and 3.6.5. In Figure 42 (A) and Figure 42 (B), the friction curve of cocoa butter (shown as average of 8 replicates) is shown together with the friction curves of the chocolates.

3.6.4 Frictional properties of the chocolate samples - PDMS surface –steady shear conditioning method

Figure 38, Figure 39, Figure 40 and Figure 41 show the Stribeck curves for the chocolates analysed in this study. Part A in each figure refers to the initial measurement and part B in each figure shows the results of the repeat measurement (run 2) on the same sample.

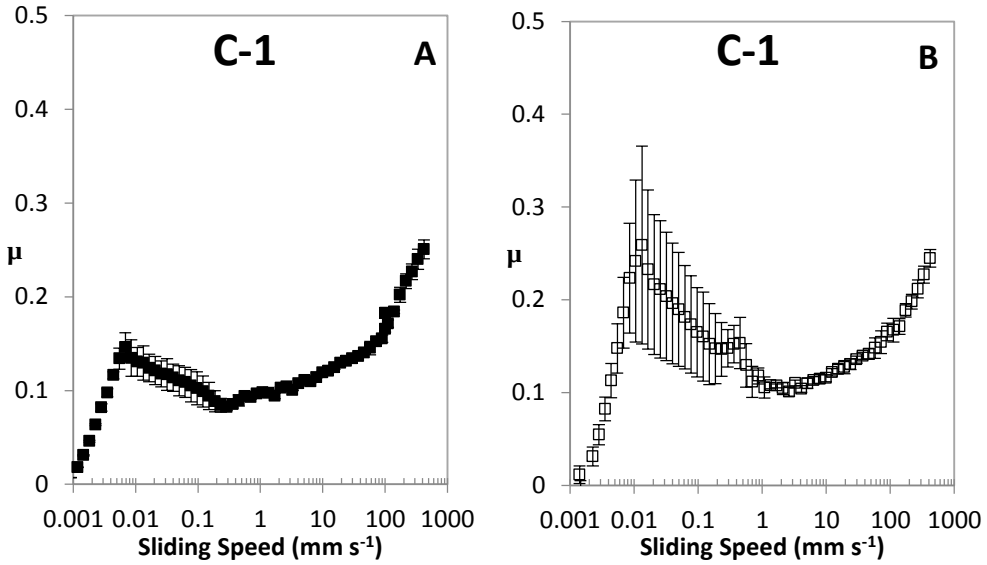

Figure 38: Friction behaviour of C-1at 37°C and 3 N applied normal force. (A) shows the results of the first measurement following conditioning at 100 mm s^{-1} and (B) shows the results of the repeat measurement (run 2) immediately started after run 1 omitting the conditioning step. Sliding speed was increased from 0.001 to 420 mm s^{-1} in 240 seconds.

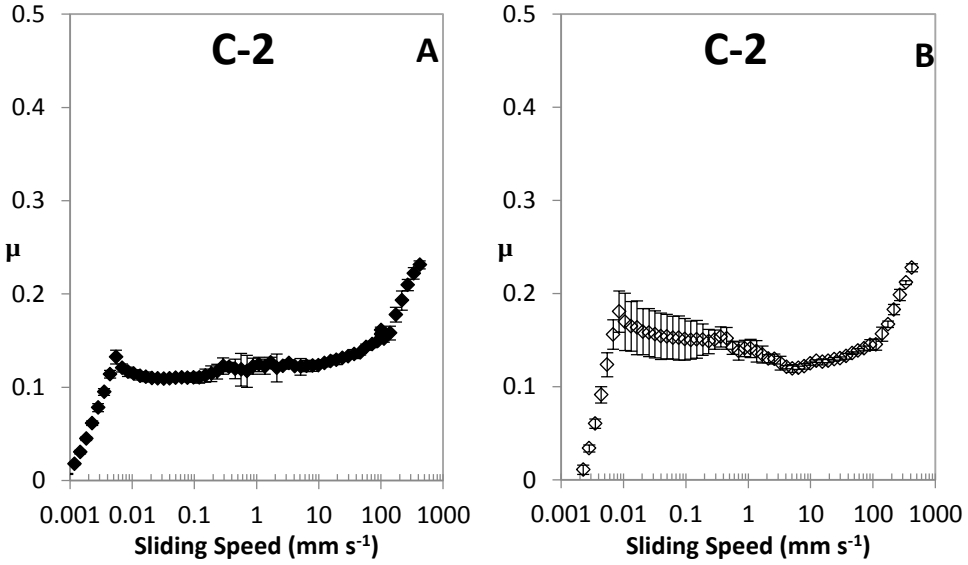

Figure 39: Friction behaviour of C-2 at 37°C and 3 N applied normal force. (A) shows the results of the first measurement following conditioning at 100 mm s^{-1} and (B) shows the results of the repeat measurement (run 2) immediately started after run 1 omitting the conditioning step. Sliding speed was increased from 0.001 to 420 mm s^{-1} in 240 seconds.

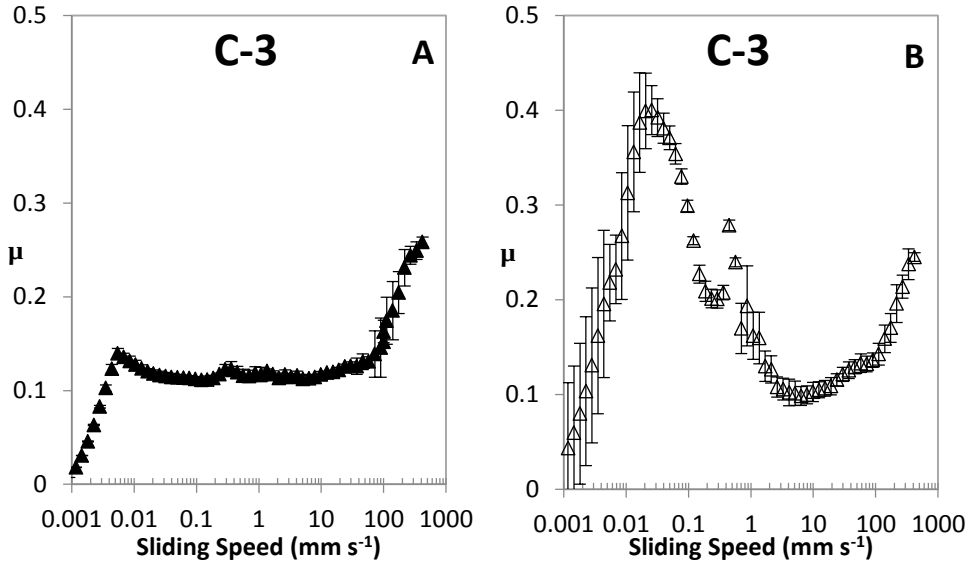

Figure 40: Friction behaviour of C-3 37°C and 3 N applied normal force. (A) shows the results of the first measurement following conditioning at 100 mm s^{-1} and (B) shows the results of the repeat measurement (run 2) immediately started after run 1 omitting the conditioning step. Sliding speed was increased from 0.001 to 420 mm s^{-1} in 240 seconds.

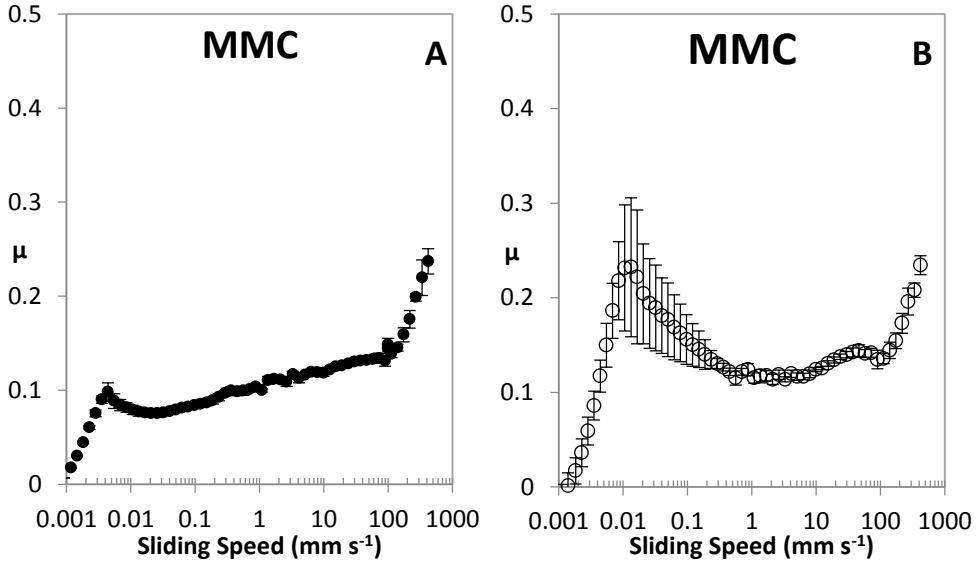

Figure 41: Friction behaviour of MMC at 37°C and 3 N applied normal force. (A) shows the results of the first measurement following conditioning at 100 mm s^{-1} and (B) shows the results of the repeat measurement (run 2) immediately started after run 1 omitting the conditioning step. Sliding speed was increased from 0.001 to 420 mm s^{-1} in 240 seconds.

The friction behaviour of the four chocolates measured with PDMS as the soft surface are similar to those found with PU surface, the maximum friction coefficient values on PDMS surfaces were slightly lower compared to those seen with PU surfaces, both in run 1 and run 2. This trend is particularly visible for C-2 in run 2, whose μ peak values lower from 0.32 on PU to 0.18 on PDMS. Differences in hardness and smoothness between the two kinds of surface are barely detectable to the touch; it could therefore be hypothesised that the different friction values could depend on the interfacial properties of the two materials. As with PU surfaces, all four chocolates tested on PDMS show clear difference in the friction profile of run 1 compared with run 2, although these differences are less high for C-2. As Gabriele *et al.* (2010) reported for fluid gel tribology, in the mixed regime only the fluid part can be entrained between the surfaces because the sliding speed is not sufficiently high to entrain the solid particles, while at higher sliding speeds the solid particles can also be entrained. The friction coefficient increase in the hydrodynamic regime seems to depend not only on the layer thickness but also on the increasing presence of solid particles. As with fluid gels, this reasoning could be applied to the melted chocolate, which contains fluid cocoa butter and particles as sugar, cocoa solids and milk powder. As stated in section 3.6.2, run 2 can show higher μ because the particles are adsorbed to the surface and they play a role in increasing μ in the mixed regime in run 2. With speed increasing, the cocoa butter is entrained again and μ decreases with increasing sliding speed. To facilitate comparison between the four chocolates, the results have been combined in Figure 42.

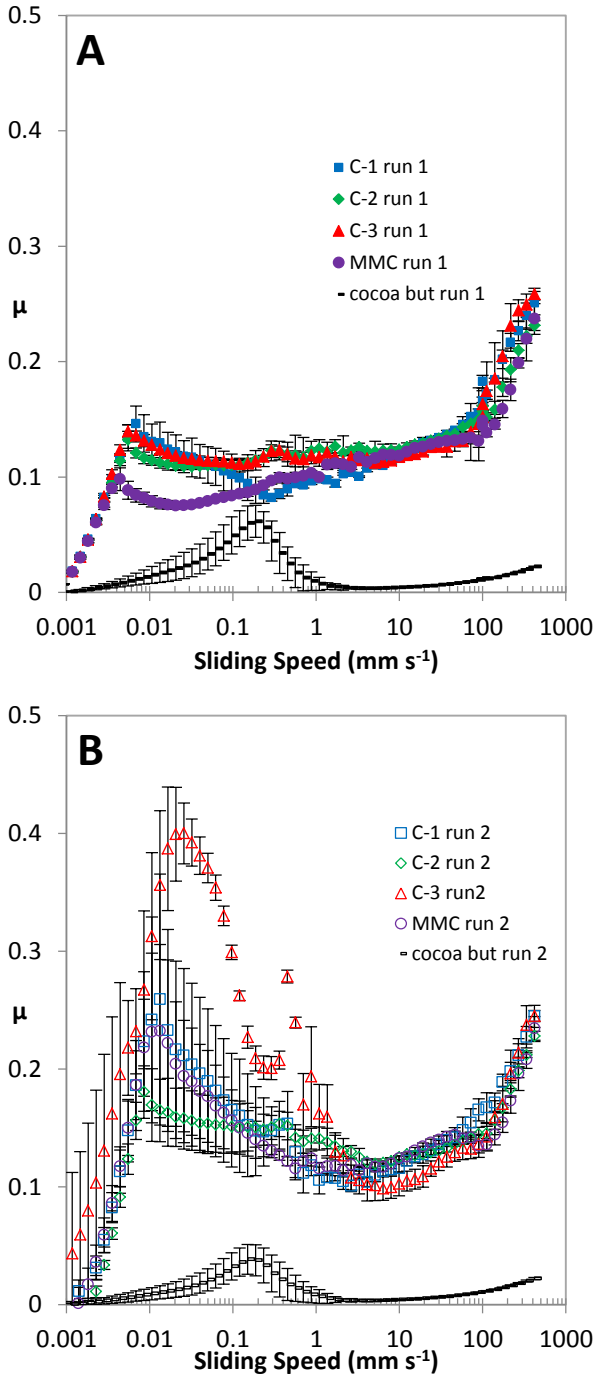

Figure 42: Combined presentation of the results shown in Figure 38, Figure 39, Figure 40 and Figure 41. The friction curves obtained with cocoa butter are also shown.

As for PU, in the chocolates analysed with PDMS, a boundary regime cannot be identified in the Stribeck curves acquired. The friction curves in Figure 42 (A), obtained after surface conditioning step, show little pronounced mixed

regime, extending only to 0.03 mm s^{-1} sliding speeds for C-2 and MMC and to 0.1 mm s^{-1} for C-3 and C-1, the latter presenting a clearer mixed regime compared to the other samples. The peak values registered in this region are around 0.15 for C-1, C-2 and C-3; MMC shows instead lower values of friction coefficient in the mixed regime in comparison to the other samples, whilst the μ values of C-2 and C-3 show an upward trend at sliding speed between 0.1 and 1 mm s^{-1}. The friction profile of the four chocolates in Figure 42 B, which corresponds to run 2, is characterised by higher friction coefficient values at sliding speeds between 0.001 and 1 mm s^{-1} and a more pronounced mixed regime compared to the friction curves in run 1. In Figure 42 B a clear mixed regime is seen, despite C-2 showing a less steep decrease compared to the other samples. From Figure 42 B it is possible to see how C-1, C-2 and C-3 have a friction behaviour which falls into the mixed regime at speed until 10 mm s^{-1}, while the mixed regime of MMC is extended at only 1 mm s^{-1}, which is the value found in run 2 for all the chocolates tested on PU surfaces. Comparing the results of run 1, MMC shows the lowest friction coefficient among the four chocolates in the mixed and elasto-hydrodynamic regime, as for PU surface test. With PDMS surface we can observe a similar trend for the other three chocolates in run 1, which overlap at the onset of the mixed regime, then C-3 and C-2 show upward trend at sliding speed between 0.1 and 1 mm s^{-1}. C-3 showed an upward trend also with PU surface in run 1. In run 2, instead, C-3 shows higher values of μ in the mixed regime compared to the other samples. In particular, at the same sliding speed range at which the upward trend is found in run 1, C-3 shows a sudden increase in μ in the mixed regime, then μ decreases again. Similar friction behaviour was reported by Gabriele *et al.* (2010) for fluid gels, where the friction coefficient increase was identified as the onset of the entrainment of the solid particles; at the sliding speed at which the increase is registered, the gap between the ball and the disk is expected to be similar to the size of the particles entrained. According to Gabriele *et al.* (2010), further increases in the sliding speed allows the entrainment of more particles, thus increasing the gap

between the surfaces above the dimensions of the particles bringing the μ value to decrease again. This mechanism could also explain the discontinuity of μ decrease in the mixed regime for C-3. However, this behaviour was not observed for the other chocolates and it might depend on the fact that the bigger particles they have compared to C-3 are more difficultly entrained in the friction zone.

The increase of the friction coefficient in C-3 was observable in all three methods used, but it was more evident on PDMS, especially in the 8 runs method.

Regarding run 2, although the standard deviation does not allow to clearly highlight differences between the samples, C-2 seems to have the lowest friction coefficient values in the mixed regime, at sliding speeds between 0.01 and 0.1 mm s^{-1}, whilst the friction curves of MMC and C-1 overlap throughout the speed range applied.

While in run 1 the values of standard deviation are low for all chocolates, they increase in run 2. This difference in levels of standard deviation might depend on the composition of the lubricant layer, which differs between run 1 and run 2. Run 1 is more related to the chocolate wetting behaviour (see section 3.6.2), with a predominant effect of the melted cocoa butter, an homogeneous system, while the friction behaviour in run 2 is influenced by the solid particles which have different size and shape, thus reducing the system homogeneity and the repeatability of the measurements.

3.6.5 Frictional properties of the chocolate samples: PDMS surface – 8 runs method

Figure 43, Figure 44, Figure 45 and Figure 46 show the Stribeck curves for the four chocolates analysed in this study. Part (A) in each figure refers to the initial measurement and part (B) in each figure shows the results of the last of eight consecutive measurements (run 8) on the same sample.

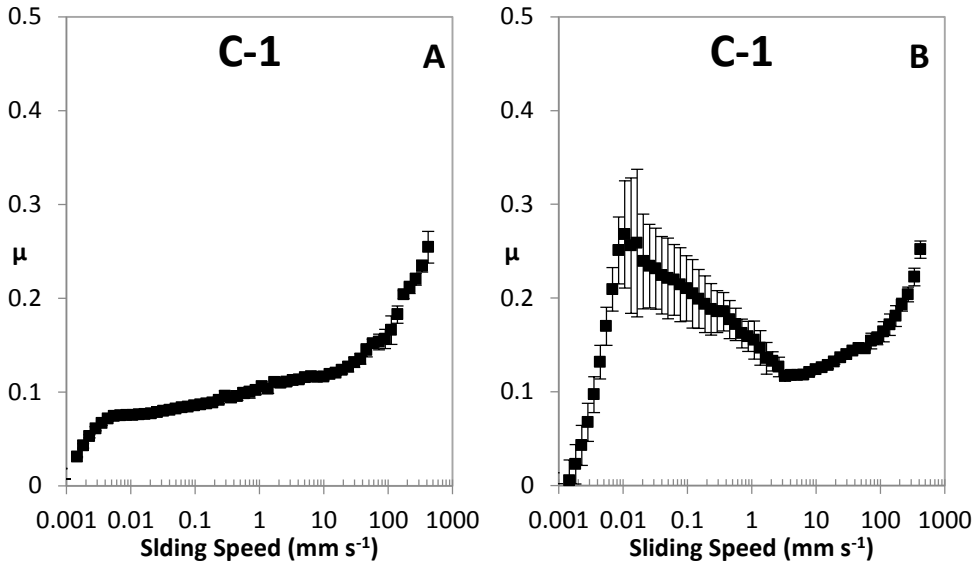

Figure 43: Friction behaviour of C-1at 37°C and 3 N applied normal force. (A) shows the results of the first measurement (run 1) in absence of conditioning step and (B) shows the results of the last of 8 consecutive measurements (run 8). Sliding speed was increased from 0.001 to 420 mm s^{-1} in 240 seconds.

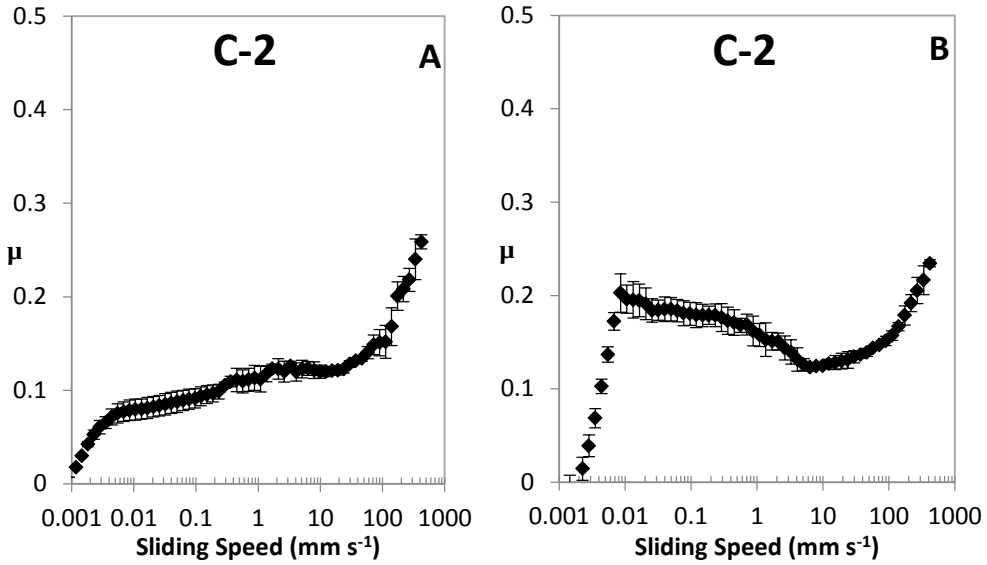

Figure 44: Friction behaviour of C-2 at 37°C and 3 N applied normal force. (A) shows the results of the first measurement (run 1) in absence of conditioning step and (B) shows the results of the last of 8 consecutive measurements (run 8). Sliding speed was increased from 0.001 to 420 mm. s^{-1} in 240 seconds

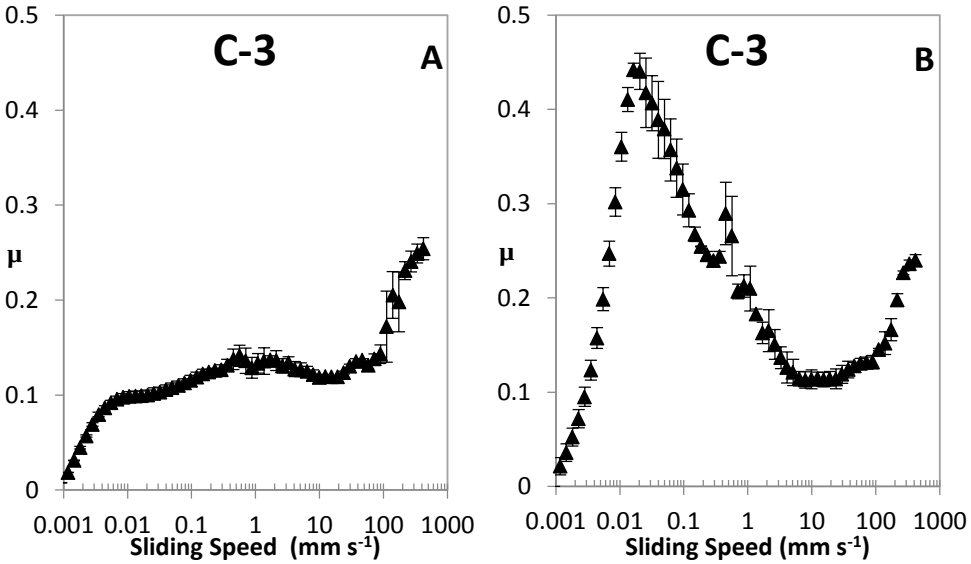

Figure 45: Friction behaviour of C-3 at 37°C and 3 N applied normal force. (A) shows the results of the first measurement (run 1) in absence of conditioning step and (B) shows the results of the last of 8 consecutive measurements (run 8). Sliding speed was increased from 0.001 to 420 mm. s^{-1} in 240 seconds.

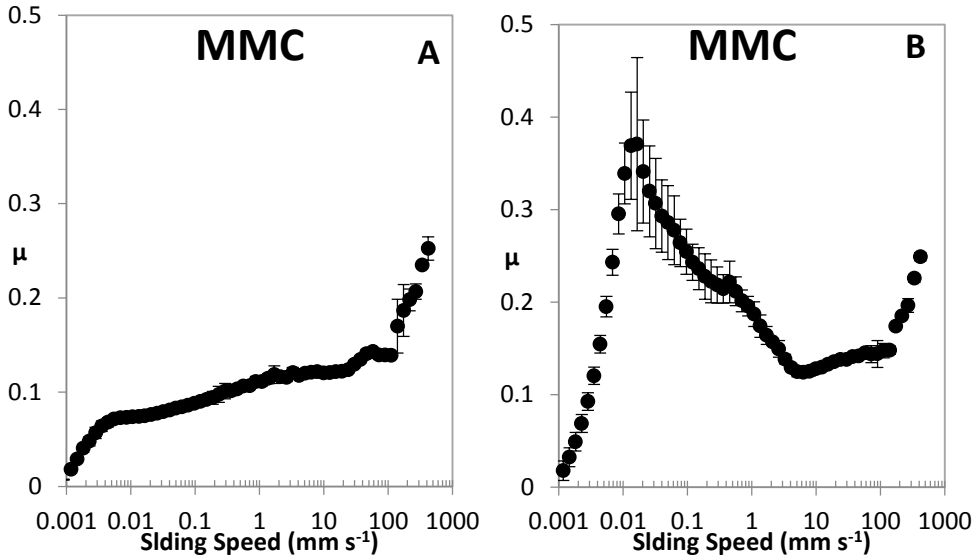

Figure 46: Friction behaviour of MMC at 37°C and 3 N applied normal force. (A) shows the results of the first measurement (run 1) in absence of conditioning step and (B) shows the results of the last of 8 consecutive measurements (run 8). Sliding speed was increased from 0.001 to 420 mm. s^{-1} in 240 seconds.

To facilitate comparison between the four chocolates, the results have been combined in Figure 47.

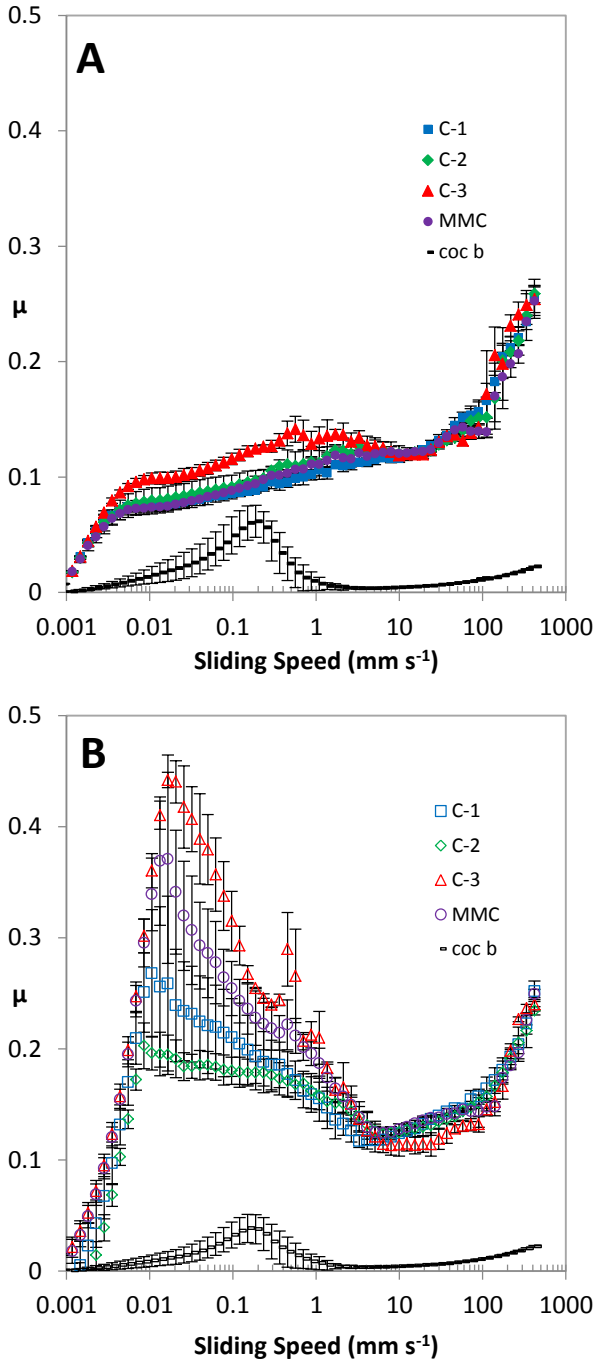

Figure 47: Combined presentation of the results shown in Figure 43 Figure 44 Figure 45 Figure 46. The friction curve obtained with cocoa butter is also shown, as average of eight replicates. The cocoa butter friction curve in (B) refers to run 2, whilst the friction curves of the chocolates refer to run 8.

In the friction curves obtained from the first measurement (run 1, Figure 47 A), which did not follow any previous conditioning step, the mixed regime is

not visible, but a steady increase in the friction coefficient, which signifies the elasto-hydrodynamic regime, is registered. An explanation of this could be that in run 1, the lack of the conditioning step, characterised by high rotating (shear) speed, does not allow the entrainment of the solid particles in the lubrication layer between the particles, so the friction coefficient is lower in the sliding speed range 0.001-0.002 mm s^{-1} in comparison to the methods with conditioning step. As for the other methods, an elastic deformation is first observed at very low sliding speed, but the chocolates then directly enter the elasto-hydrodynamic regime at already 0.002 mm s^{-1} sliding speed.

At sliding speeds around 100 mm s^{-1} for run 1 and run 8, an increase in the friction curves slope is observed and this is the beginning of the hydrodynamic regime (Carvalho-da-Silva *et al.*, 2013). In run 1, the friction curves of C-1, C-2 and MMC generally overlap throughout the sliding speed range, whilst C-3 gives higher friction coefficient values between 0.003 and 1 mm s^{-1}. In the friction curves at run 8, depicted in Figure 47 B, C-3 shows a sudden increase in μ at sliding speeds just below 1 mm s^{-1}. The results at sliding speeds above 10 mm s^{-1} coincide for both run 1 and run 8. In Figure 47 B, it is possible to see different friction behaviour between the four chocolate samples, in the sliding speed range from 0.01 to 1 mm s^{-1}, which corresponds to the mixed regime, although the standard deviation does not consent to completely distinguish the four chocolates friction behaviours.

No important differences in the friction curves were observed between run 8 in the 8 runs method and run 2 in the 100 mm s^{-1} surface conditioning step method, with the exception of MMC, which showed higher friction coefficient values and a more extended mixed regime compared to surface conditioning method run 2.

Surface activity of the various chocolate components influences its friction behaviour (Carvalho-da-Silva et al. 2013), but the mechanisms that regulate chocolate lubrication have not been clearly identified so far. In general, the friction properties of foods have seen to be related to the combination of a

series of factors like fat content, emulsifier type (Douaire *et al*., 2014), fat constitution as well as particle size (Luengo *et al.*, 1997). According to de Wijk and Prinz (2005) particles of bigger size cause higher friction in comparison with smaller particles.

With respect to the 8 runs method, the one that gave the greatest differences between the chocolates, considering particle size values (D_{90}) of the four chocolates, the relationship seems to be instead that bigger particle size gives lower friction, although C-2 and C-1 do not show this relationship. Even though bigger particles were found to cause higher friction compared to smaller particles (de Wijk and Prinz, 2005), it is presumable that bigger particles are more difficult to entrain into the friction zone, and they contribute to friction by a smaller amount, whilst cocoa butter can be more easily entrained, so there is higher concentration of cocoa butter in the friction zone, and friction is lowered due to lubricating properties of fat. As mentioned in section 3.6.2, the friction in run 1 should be principally regulated by the chocolate wetting behaviour, whilst in the following runs the role of solid particles in determining the values of friction coefficient gains importance. Despite so, particle size could also explain why C-3 showed the highest μ in run 1, based on the fact it has the smallest value of D_{90}, thus the smaller particles can be more easily entrained and the solids concentration in the friction zone is higher in C-3 than in the other chocolates.

Beside particles size, another factor affecting the friction behaviour of chocolate is the presence and characteristics of surface active molecules such as proteins. The protein profile of the chocolates is different, as shown in section 3.1, and this may be related to different level of hydrophobicity of the proteins between the chocolates, with an effect on the way the proteins interact with fat or with the friction surfaces. In particular, protein adhesion to specific friction surfaces was considered by different authors to affect the friction behaviour of foods and food-like systems. Sibarani *et al.* (2007) found a higher level of adhesion of proteins on more hydrophobic surfaces (such as

PDMS) than at less hydrophobic surfaces (such as Polyvinylcloride), whilst Heuberger *et al.* (2005) and Widmer *et al.* (2001) reported higher protein adherence to more hydrophilic surfaces than to more hydrophobic surfaces. This clearly depends on the type of protein and surface material.

Also protein concentration was reported to affect the friction. An increase in friction was measured with increasing protein content on hydrophilic surfaces by Karuppiah *et al.* (2006), whilst higher values of friction were measured with increasing protein content on hydrophobic surfaces by Dresselhuis *et al.* (2008). With regard to this study, the differences in protein content between the four chocolate analysed are probably not sufficient for a relationship between μ in the mixed regime and protein content to be established. Whereas it is conceivable to hypothesize there being a relationship between the role of protein characteristics on friction. Proteins characteristics can be influenced by the manufacturing process; a heating step applied to the proteins in the presence of sugar may enhance the protein hydrophobicity. Considering the 8 runs method on PDMS, which shows clearer differences between the samples, is it possible to observe how C-1and C-2 show lower friction in the mixed regime, whilst C-3 and MMC show higher friction, and the protein profile between these two "groups" of samples is different, as shown by the SDS-PAGE results in section 3.1. Thus the relationship between proteins and surfaces needs to be investigated in order to understand how their hydrophobicity can affect the friction of the chocolates. Overall, in order to have a deeper understanding of how the characteristics of the single ingredients are linked to the chocolate friction behaviour, future work should include manufacture of chocolate models with different formulations.

3.7 Chocolate bolus friction properties

The friction properties of the *in-vitro* boluses were determined and compared to the friction data available for *in-vivo* boluses prepared from the same four chocolates. As explained in section 2.8, an attempt was made to

match the microstructure of the *in-vitro* boluses to the microstructure of the in vivo boluses. Based on particle size data and micrographs available for the in vivo boluses (not included since data acquired by third party), the emulsification regime of chocolate with water was set as stated in section 2.8. Micrographs of the in vitro boluses are shown in Figure 48.

From a visual observation of the micrographs of the four chocolate emulsions, the particles have the same order of magnitude as the particle size data acquired in the in vivo bolus. C-1and C-2 have similar micrographs whilst C-3 shows smaller particles compared to C-1 and C-2; MMC shows instead the biggest droplets among the four emulsions and also flocculated cocoa solids agglomerates are visible. These images give an idea of how the emulsions generally appear but PSD analysis is required to get more complete information and to compare it with the results on in vivo bolus.

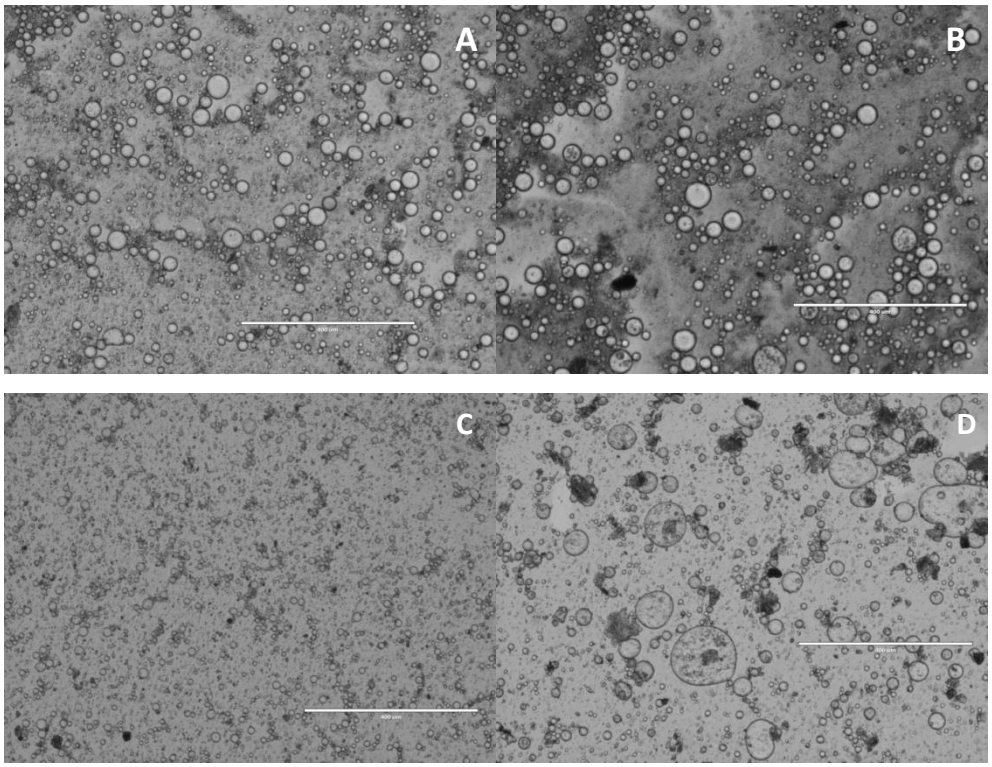

Figure 48: Micrographs of C-1(A), C-2 (B), C-3 (C) and MMC (D) in vitro bolus. The emulsions were obtained at 6000 RPM for 40 s, by using a disperser (Ultra Turrax, T 18 basic, IKA). The size of the scale (400 µm) is shown in the pictures.

The friction curves obtained for the in vitro bolus for the four chocolates are depicted in Figure 49.

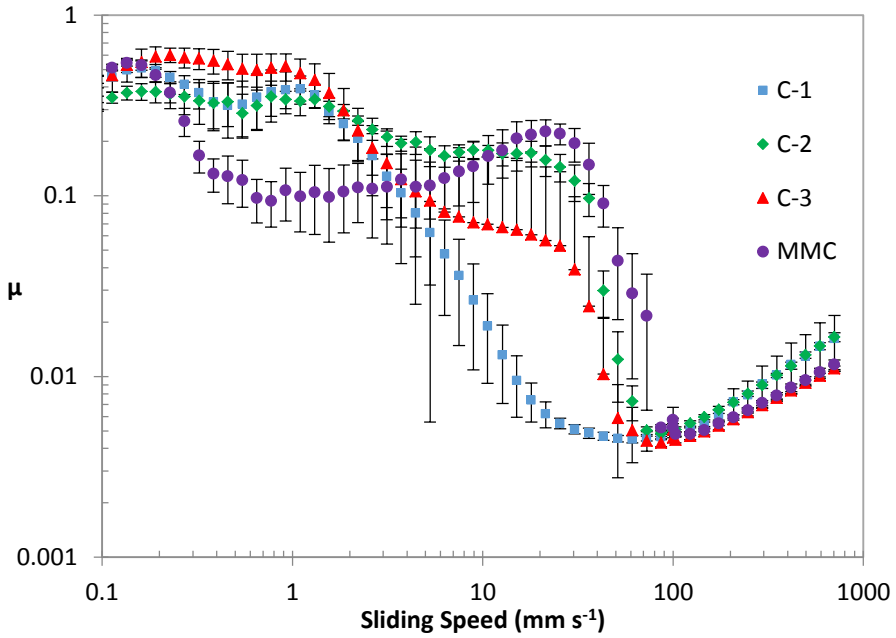

Figure 49: Friction behaviour of C-1, C-2, C-3 and MMC in vitro bolus at 40°C and 3 N applied normal load. Sliding speed was increased from 0.05 to 705 mm s^{-1}. The friction coefficient μ is plotted as a function of sliding speed (mm s^{-1})

The friction curves of the C-1, C-3 and MMC in vitro boluses show similar values of friction coefficient at sliding speed between 0.1 and 0.2 mm s^{-1}, while C-2 bolus has slightly lower friction coefficient. C-2 and C-3 boluses have quite constant friction coefficient until 2 mm s^{-1} and this trend was considered as the boundary regime. Also C-1 shows similar trend for the friction coefficient in the sliding speed range 0.1-2 mm s^{-1}, despite the variability is slightly higher than in C-2 and C-3. However, that trend was considered to represent the boundary regime. C-1and C-2 show similar friction coefficient in the boundary regime, at sliding speed over 0.3 mm s^{-1}, while C-3 has slightly higher values. MMC has instead much less extended boundary regime compared to the other boluses. While in the mixed regime C-1 shows constant decrease of the friction coefficient until reaching

minimum value at around 70 mm s^{-1}, for C-3 and C-2 the slope in the mixed regime is not constant, both showing a discontinuity between 8 and 30 mm s^{-1}. MMC bolus behaviour significantly differs from the other boluses since a second peak is observable at sliding speed of 30 mm s^{-1}. Although the four *in-vitro* boluses friction curves differ between them, the minimum friction is observable at speed between 70-100 mm s^{-1} for all the chocolate boluses, and at this speed the elasto-hydrodynamic regime is reached. At higher speed the friction coefficient increases and the boluses enter the hydrodynamic regime. In this regime it is possible to observe how C-1 and C-2 friction curves overlap, and the same occurs for C-3 and MMC but they show lower friction coefficient compared to C-1 and C-2. This can be explained by the higher viscosity that C-1 and C-2 showed compared to C-3 and MMC.

Overall, the friction curves of the *in-vitro* boluses differ from the Stribeck curve especially in the mixed regime, where only C-1 shows constant decrease. MMC instead shows a clear second peak before reaching the elasto-hydrodynamic regime. This second peak might be due to the entrainment of particles such as the droplets with the biggest size in the friction zone. Even though the droplet size of the emulsions is not clearly correlated to the differences in friction behaviour, fat droplets with the biggest size might require higher sliding speeds to be entrained in the friction zone, increasing the friction coefficient before breaking and spreading on the surface, with lubrication effect and consequent decrease of the friction coefficient.

At the moment it is not clear which factors influence the *in-vitro* bolus friction and how they cause the differences between the samples. Since the fat content is comparable between the four chocolate boluses, it cannot be considered to differentiate the friction behaviour. Comparing the friction curves of the in *in-vitro* boluses with the bulk chocolate curves tested on PDMS following 100 mm s^{-1} run-in step, and in particular in run 1 (see Figure 42 A, section 3.6.4), the friction coefficient in the boluses is higher than in

the bulk chocolates. A possible explanation of this lies in the different nature of the continuous phase, which is water in the case of the bolus, while it is fat in the bulk chocolate. Higher measured friction of an emulsion compared to that of the respective non-emulsified fat was previously reported (Dresselhuis *et al.*, 2007). The explanation of a more extended boundary regime may lie in the lubricant activity of the fat. While in the bulk chocolate the fat represents the continuous phase, in the emulsified chocolate the fat represents the dispersed phase. For this reason, the availability of the fat to be spread on the surface (and act as lubricant) is reduced compared to bulk chocolate, because fat is in lower amount and it is also immerged into a polar environment, the droplets need to be broken before they can spread on the sliding surfaces and the effect of fat in reducing the friction coefficient is observed at higher sliding speed. In the bulk chocolate, the fat should be instead readily available and its wetting action on the hydrophobic surface may be more effective. The boluses friction coefficient is instead lower at higher speeds, when the boluses friction curves are in the elasto-hydrodynamic and hydrodynamic regimes. This may depend on the lower viscosity that is expected to characterise the *in-vitro* boluses compared to the bulk chocolates. If for bulk chocolate the different particle size can affect the friction coefficient, it is not clear if the particle size of the emulsion plays the same role in the emulsified chocolate. At the moment clear correlations between the friction behaviour in bulk chocolate and emulsified chocolate cannot be identified.

In order to see if the friction data on *in-vitro* boluses prepared as described in section 2.8 are comparable with the friction behaviour of *in-vivo* boluses, the friction curves of the *in-vitro* and *in-vivo* boluses were compared, as shown in Figure 50.

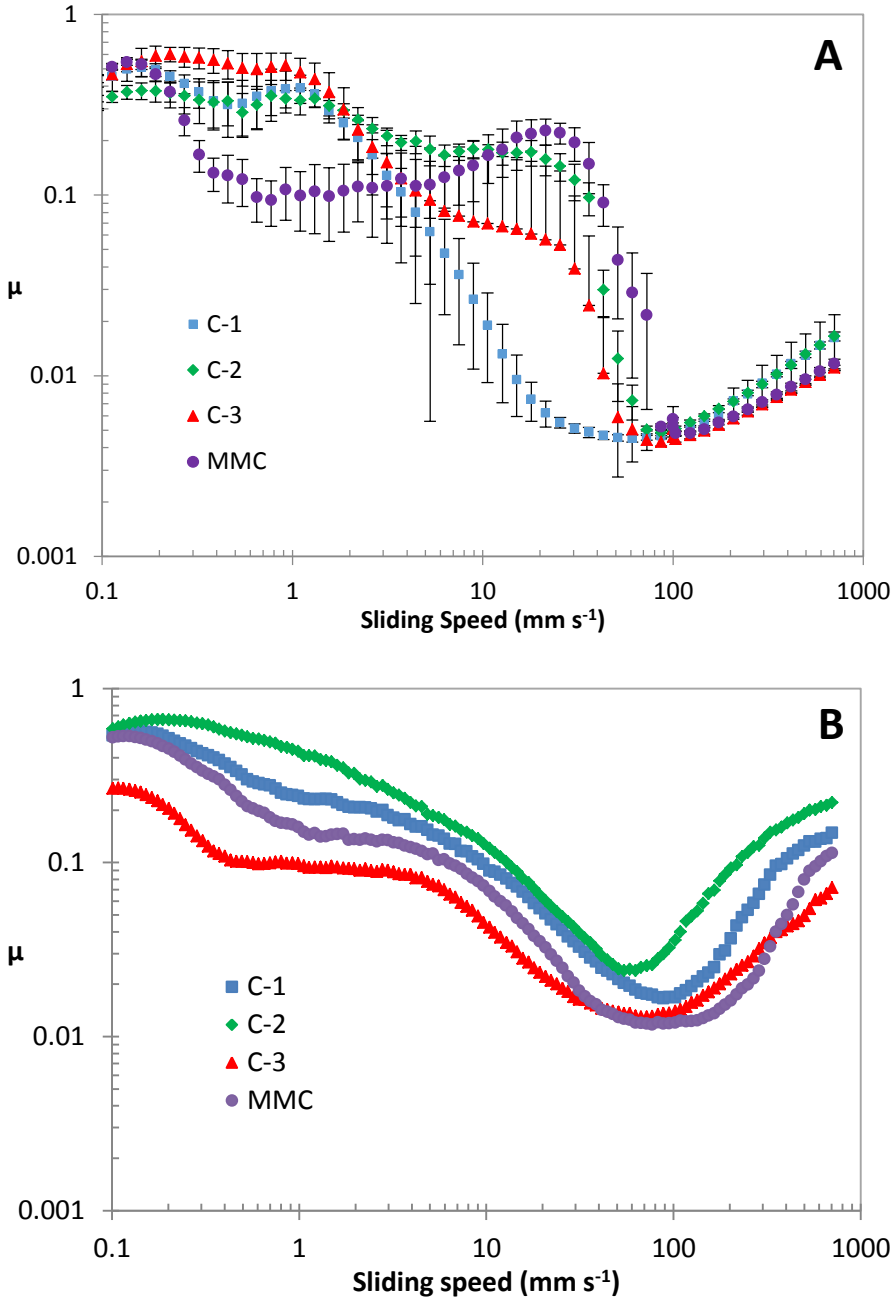

Figure 50: Friction curves for the *in-vitro* bolus obtained in this study (A) and *in-vivo* bolus available (B) for C-1, C-2, C-3 and MMC. The friction curves in both the methods were obtained following the same procedure described in section 2.8. Sample legend is shown in (A).

As it is possible to observe in Figure 50, the friction data are similar in magnitude although shape and relative order of the curves is different for the two types of boluses. No second maximum friction coefficient is observable in the case of the *in-vivo* bolus and the curves appear smoother;

the minimum friction coefficient is instead reached roughly at the same sliding speed, at which all of the boluses reach the elasto-hydrodynamic regime. C-3, C-2 and C-1 *in-vitro* boluses show more extended boundary regime compared to the respective *in-vivo* boluses, whilst MMC has comparable boundary regime extension in the two types of bolus.

The lower friction coefficient shown by the *in-vitro* boluses compared to the *in-vivo* boluses in the hydrodynamic regime may be determined by the different viscosity of the continuous phase, constituted in one case by water and in the other one by saliva. Since saliva is marginally more viscous than water, it may increase the viscosity of the whole emulsion.

In conclusion, from the differences observed between the friction curves of the *in-vitro* and *in-vivo* boluses, a role of saliva in regulating the friction properties of the bolus is not excluded. At the same time, the role of particle size is still not clear and it might affect the friction properties and for this PSD data should be acquired from the *in-vitro* boluses. Furthermore, although the emulsions show particle size of the same order of magnitude, the process of emulsification between the in-vitro and the in-vivo boluses are different and this may affect the structure of the interface.

In order to have a deeper understanding of the factors and the mechanisms that affect the bolus microstructure and its friction behaviour, including the possible role of saliva in affecting the friction, the development of chocolate model boluses, which take into account emulsifiers and salivary proteins, should be considered as next step.

The microstructure of the *in-vitro* bolus developed for this study may still differ in some way from the microstructure of the *in-vivo* bolus and the localisation of the chocolate ingredients in the two types of bolus should be inspected by advanced microscopy and computational analysis.

4 Overall conclusions and next steps

The four chocolates exhibit different material properties which can be related to the manufacturing procedure and the ingredients used. The different values of hardness and viscosity shown by the chocolates may be explained by different amount of milk fat in the continuous fat phase between the chocolates, and this can be related to different types of the milk ingredient utilised. Furthermore, differences in the chocolate manufacturing process may be reflected also in the different protein profile as suggested by SDS-PAGE analysis. C-3 and MMC are the only chocolates which show the β-lg and α-la bands. The lack of the β-lg and α-la bands in C-1 and C-2 instead indicates that the nature of the milk ingredient used in the formulation is different. The melting properties of the chocolates measured with the DSC indicate that the fat profile of the four chocolates is similar. Regarding chocolate particle size, C-3 and MMC have smaller values compared to C-1 and C-2, and the trend observed in the friction tests on PDMS, especially in run 8 of the 8 runs test, seems to be that of lower particle size is related to higher friction. Regarding instead the meltdown behaviour, the four chocolates showed less difference, and the difference between the samples was not related to any specific characteristic of the chocolates, and differences may rather depend on the combination of more factors determined by the formulation and the manufacturing process.

Generally, for some of the material properties investigated in this study, it is possible to see how the trend is that of C-1 and C-2 on one hand side and C-3 and MMC on the other. This trend can be related to the different ingredients utilised for the chocolates, such as the type of milk, and it may also indicate similarities in the manufacturing process between the two “groups” of chocolates.

In order to have a deeper understanding about the role of the ingredients in affecting the material properties measured in this study, the development of model chocolates to test the influence of type and amount of the different ingredients should be next steps.

The chocolate *in-vitro* boluses friction behaviour was different from that of the bulk chocolate, so the friction properties of the bulk chocolate are modified by the emulsification process. At the same time the friction curves of the *in-vitro* boluses differed from those of the *in-vivo* boluses, but the order of magnitude of the friction coefficient and the sliding speed at which the friction coefficient reached the minimum were comparable. The different friction behaviour between the two types of bolus may depend on differences in microstructure at the interface and the role of saliva in structuring the interface cannot be excluded at the moment, so further study is required with the aim of replacing the *in-vivo* bolus with the *in-vitro* bolus for the evaluation of the friction properties of the oral processed chocolate. For this reason, the localisation of the chocolate ingredients in the two types of bolus should be inspected by advanced microscopy and computational analysis.

5 References

AFOAKWA, E. O., PATERSON, A., FOWLER, M. & VIEIRA, J. 2008a. Characterization of melting properties in dark chocolates from varying particle size distribution and composition using differential scanning calorimetry. *Food Research International,* 41**,** 751-757.

AFOAKWA, E. O., PATERSON, A., FOWLER, M. & VIEIRA, J. 2008b. Relationship between rheological, textural and melting properties of dark chocolate as influenced by particle size distribution and composition. *European Food Research and Technology,* 227**,** 1215-1223.

AHMED, J. & RAMASWAMY, H. S. 2006. Viscoelastic properties of sweet potato puree infant food. *Journal of Food Engineering,* 74**,** 376-382.

BASCH, J. J., DOUGLAS, F. W. J., PROCINO, L. G., HOLSINGER, V. H. & FARRELL, H. M. J. 1985. Quantitation of Caseins and Whey Proteins of Processed Milks and Whey Protein Concentrates, Application of Gel Electrophoresis, and Comparison with Harland-Ashworth Procedure. *Journal of Dairy Science,* 68.

BECKETT, T. S. 2008. *The Science of chocolate*, The Royal Society of Chemistry.

BOLENZ, S., MEIER, J. S. R. & SCHÄPE, R. 2000. Sensorische Parameter im Fokus. *Zucker Susswarenwirtschaft,* 53 309–314.

BRIGHENTI, M., GOVINDASAMY-LUCEY, S., LIM, K., NELSON, K. & LUCEY, J. A. 2008. Characterization of the rheological, textural, and sensory properties of samples of commercial US cream cheese with different fat contents. *Journal of Dairy Science,* 91**,** 4501-4517.

CAMPBELL, L. B. & PAVLASEK, S. J. 1987. Dairy products as ingredients in chocolate and confections *AGRIS,* 41.

CARVALHO-DA-SILVA, A. M., VAN DAMME, I., TAYLOR, W., HORT, J. & WOLF, B. 2013. Oral processing of two milk chocolate samples. *Food & Function,* 4**,** 461-469.

CASSIN, G., HEINRICH, E. & SPIKES, H. A. 2001. The Influence of Surface Roughness on the Lubrication Properties of Adsorbing and Non-Adsorbing Biopolymers. *Tribology Letters,* 11**,** 95-102.

CIVILLE, G. V. & SZCZESNIAK, A. S. 1973. Guidelines to training a texture profile panel. *Journal of Texture Studies,* 4**,** 204–223.

CUTLER, A. N., MORRIS, E. R. & TAYLOR, L. J. 1983. Oral Perception of Viscosity in Fluid Foods and Model Systems. *Journal of Texture Studies,* 14**,** 377-395.

DAN, H., OKAMOTO, M., WADA, Y., DAN, I. & KOHYAMA, K. 2007. First bite for hardness judgment as haptic exploratory procedure. *Physiology & Behaviour,* 92**,** 601-610.

DE GRAEF, V., DEPYPERE, F., MINNAERT, M. & DEWETTINCK, K. 2011. Chocolate yield stress as measured by oscillatory rheology. *Food Research International,* 44**,** 2660-2665.

DE HOOG, E. H. A., PRINZ, J. F., HUNTJENS, L., DRESSELHUIS, D. M. & VAN AKEN, G. A. 2006. Lubrication of Oral Surfaces by Food Emulsions: the Importance of Surface Characteristics. *Journal of Food Science,* 71**,** E337-E341.

DE VICENTE, J., STOKES, J. R. & SPIKES, H. A. 2005. The Frictional Properties of Newtonian Fluids in Rolling–Sliding soft-EHL Contact. *Tribology Letters,* 20**,** 273-286.

DE WIJK, R. A. & PRINZ, J. F. 2005. The role of friction in perceived oral texture. *Food Quality and Preference,* 16**,** 121-129.

DE WIJK, R. A., VAN GEMERT, L. J., TERPSTRA, M. E. J. & WILKINSON, C. L. 2003. Texture of semi-solids; sensory and instrumental measurements on vanilla custard desserts. *Food Quality and Preference,* 14**,** 305-317.

DO, T. A., HARGREAVES, J. M., WOLF, B., HORT, J. & MITCHELL, J. R. 2007. Impact of particle size distribution on rheological and textural properties of chocolate models with reduced fat content. *Journal of Food Science,* 72**,** E541-E552.

DRESSELHUIS, D., DEHOOG, E., COHENSTUART, M. & VANAKEN, G. 2008. Application of oral tissue in tribological measurements in an emulsion perception context. *Food Hydrocolloids,* 22**,** 323-335.

DRESSELHUIS, D. M., KLOK, H. J., STUART, M. A. C., DE VRIES, R. J., VAN AKEN, G. A. & DE HOOG, E. H. A. 2007. Tribology of o/w emulsions under mouth-like conditions: Determinants of friction. *Food Biophysics,* 2**,** 158-171.

FARRELL, H. M., JR., JIMENEZ-FLORES, R., BLECK, G. T., BROWN, E. M., BUTLER, J. E., CREAMER, L. K., HICKS, C. L., HOLLAR, C. M., NG-KWAI-HANG, K. F. & SWAISGOOD, H. E. 2004. Nomenclature of the proteins of cows' milk--sixth revision. *Journal of Dairy Science,* 87**,** 1641-1674.

FULL, N. A., REDDY, S. Y., DIMICK, P. S. & ZIEGLER, G. R. 1996. Physical and sensory properties of milk chocolate formulated with anhydrous milk fat fractions. *Journal of Food Science,* 61**,** 1068-1073.

GABRIELE, A., SPYROPOULOS, F. & NORTON, I. T. 2010. A conceptual model for fluid gel lubrication. *Soft Matter,* 6**,** 4205-4213.

GIASSON, S., ISRAELACHVILI, J. & YOSHIZAWA, H. 1997. Thin Film Morphology and Tribology Study of Mayonnaise. *Journal of Food Science,* 62.

GLICERINA, V., BALESTRA, F., ROSA, M. D. & ROMANI, S. 2013. Rheological, textural and calorimetric modifications of dark chocolate during process. *Journal of Food Engineering,* 119**,** 173-179.

GREEN, M. R. & PASTEWKA, J. W. 1976. Molecular Weights of Three Mouse Milk Caseins by Sodium Dodecyl Sulfate-Polyacrylamide Gel Electrophoresis and κ-Like Characteristics of a Fourth Casein. *Journal of Dairy Science* 59**,** 1738-1745.

GREENAWAY, R. E. 2010. *Psychorheology of skin cream. PhD thesis.* University of Nottingham.

GUINARD, J. X. & MAZZUCCHELLI, R. 1999. Effects of sugar and fat on the sensory properties of milk chocolate: descriptive analysis and instrumental measurements. *Journal of the Science of Food and Agriculture,* 79**,** 1331-1339.

HARTEL, R. W. 2001. *Crystallization in Food,* Gaithersburg, USA, Aspen Publishers Inc.

HEUBERGER, M. P., WIDMER, M. R., ZOBELEY, E., GLOCKSHUBER, R. & SPENCER, N. D. 2005. Protein-mediated boundary lubrication in arthroplasty. *Biomaterials,* 26**,** 1165-73.

IOCCC 2000. Intl Office of Cocoa CaSCI. Viscosity of cocoa and chocolate products. Analytical method 46. CABISCO, rue Defacqz 1, B-100 Bruxelles, Belgium.

JOHANSSON, D. & BERGENSTAHL, B. 1992. The Influence of Food Emulsifiers on Fat and Sugar Dispersions in Oils .2. Rheology, Colloidal Forces. *Journal of the American Oil Chemists Society,* 69**,** 718-727.

JOHNSON, S. A., GORMAN, D. M., ADAMS, M. J. & BRISCOE, B. J. 1993. The Friction and Lubrication of Human Stratum-Corneum. *Thin Films in Tribology,* 25**,** 663-672.

KARUPPIAH, K. S. K., SUNDARARAJAN, S., XU, Z.-H. & LI, X. 2006. The effect of protein adsorption on the friction behavior of ultra-high molecular weight polyethylene. *Tribology Letters,* 22**,** 181-188.

KEOGH, K., MURRAY, C., KELLY, J. & O'KENNEDY, B. 2004. Effect of the particle size of spray-dried milk powder on some properties of chocolate. *Le Lait,* 84**,** 375-384.

KEOGH, K., TWOMEY, M., O'KENNEDY, B. & MULVIHILL, D. 2002. Effect of milk composition on spray-dried high-fat milk powders and their use in chocolate. *Le Lait,* 82 531–539.

KEOGH, K. M., MURRAY, C. A. & O'KENNEDY, B. T. 2003. Effects of selected properties of ultrafiltered spray-dried milk powders on some properties of chocolate. *International Dairy Journal,* 13**,** 719-726.

KIM, E. H. J., CORRIGAN, V. K., WILSON, A. J., WATERS, I. R., HEDDERLEY, D. I. & MORGENSTERN, M. P. 2012. Fundamental Fracture Properties Associated with Sensory Hardness of Brittle Solid Foods. *Journal of Texture Studies,* 43**,** 49-62.

LE REVEREND, B. J. D., FRYER, P. J. & BAKALIS, S. 2009. Modelling crystallization and melting kinetics of cocoa butter in chocolate and application to confectionery manufacturing. *Soft Matter,* 5**,** 891-902.

LEE, S., HEUBERGER, M., ROUSSET, P. & N.D., S. 2002. Chocolate at a Sliding Interface *Journal of Food Science,* 67.

LIANG, B. & HARTEL, R. W. 2004. Effects of milk powders in milk chocolate. *Journal of Dairy Science,* 87**,** 20-31.

LUENGO, G., TSUCHIYA, M., HEUBERGER, M. & ISRAELACHVILI, J. 1997. Thin Film Rheology and Tribology of Chocolate. *Journal of Food Science,* 62**,** 767-772, 812.

MALONE, M. E., APPELQVIST, I. A. M. & NORTON, I. T. 2003. Oral behaviour of food hydrocolloids and emulsions. Part 2. Taste and aroma release. *Food Hydrocolloids,* 17**,** 775-784.

MCFARLANE, I. 1999. Instrumentation. *In:* BECKETT.T.STEPHEN (ed.) *Industrial Chocolate Manufacture and Use.* New York: Chapman & Hall.

PRAKASH, S., TAN, D. D. Y. & CHEN, J. 2013. Applications of tribology in studying food oral processing and texture perception. *Food Research International,* 54**,** 1627-1635.

RICHARDSON, R. K., MORRIS, E. R., ROSS-MURPHY, S. B., TAYLOR, L. J. & DEA, L. C. M. 1989. Characterization of the perceived texture of thickened systems by dynamic viscosity measurements. *Food Hydrocolloids,* 3**,** 175-191.

SERVAIS, C., RANC, H. & ROBERTS, I. D. 2004. Determination of chocolate viscosity *Journal of Texture Studies,* 34**,** 467-497.

SIBARANI, J., TAKAI, M. & ISHIHARA, K. 2007. Surface modification on microfluidic devices with 2-methacryloyloxyethyl phosphorylcholine polymers for reducing unfavorable protein adsorption. *Colloids and Surfaces B: Biointerfaces,* 54**,** 88-93.

SPEARING, N. 2007. *The effect of fat on the texture of chocolate milk [PhD thesis].* School of Biosciences—Division of Food Sciences. The Univ. of Nottingham.

SZCZESNIAK, A. S. 1963. Classification of textural characteristics. *Journal of Food Science,* 28**,** 385-389.

SZCZESNIAK, A. S. 1979. Classification of mouthfeel characteristics of beverages. *In:* (ED.), P. S. (ed.) *Food texture and rheology.* London: Academic Press.

TABOURET, T. 1987. Detection of Fat Migration in a Confectionery Product. *International Journal of Food Science and Technology,* 22**,** 163-167.

TAYLOR, J. E., VAN DAMME, I., JOHNS, M. L., ROUTH, A. F. & WILSON, D. I. 2009. Shear rheology of molten crumb chocolate. *Journal of Food Science,* 74**,** E55-E61.

VAN DER VAART, K., DEPYPERE, F., GRAEF, V. D., SCHALL, P., FALL, A., BONN, D. & DEWETTINCK, K. 2013. Dark chocolate's compositional effects revealed by oscillatory rheology. *European Food Research and Technology,* 236**,** 931-942.

VIGNOLLES, M.-L., JEANTET, R., LOPEZ, C. & SCHUCK, P. 2007. Free fat, surface fat and dairy powders: interactions between process and product. A review. *Le Lait,* 87**,** 187-236.

WALTER, P. & CORNILLON, P. 2001. Influence of Thermal Conditions and Presence of Additives on Fat Bloom in Chocolate. *Journal of the American Oil Chemists' Society,* 78**,** 927-932.

WALTER, P. & CORNILLON, P. 2002. Lipid migration in two-phase chocolate systems investigated by NMR and DSC. *Food Research International,* 35**,** 761-767.

WELLS, M. 2009. Controlling the rheology of chocolate and fillings. *In:* TALBOT, G. (ed.) *Science and Technology of Enrobed and Filled Chocolate, Confectionery and Bakery Products.* Woodhead Publishing.

WIDMER, M. R., HEUBERGER, M. P., VÖRÖS, J. & SPENCER, N. D. 2001. Influence of polymer surface chemistry on frictional properties under protein-lubrication conditions: implications for hip-implant design. *Tribology Letters,* 10**,** 111-116.

WILLE, R. L. & LUTTON, E. S. 1966. Polymorphism of Cocoa Butter. *Journal of the American Oil Chemists Society,* 43**,** 491-496.

WINOPAL, R. A., DROBNY, L. & SCHNEIDER-HÄDER, B. 2005. Instrumental sensory testing in the food industry Part 2: Mechanical texture analysis of foods. . *DLG-Expert report 3/2015.*

WOLLNY, K. 2005. Determining the yield point and viscosity of chocolate.: Anton Paar.

ZIEGLER, H. R. & HOGG, R. 2009. Particle Size Reduction. *In:* BECKETT.T.STEPHEN (ed.) *Industrial Chocolate Manufacture and Use.* York: Wley-Blackwell.